Fat-depot specific differences in adipose tissue inflammation in the setting of obesity and insulin resistance

Eirik Nordahl-Pedersen

This thesis is submitted in partial fulfilment of the requirements for the degree of Master of Science

Department of Biological Sciences

Hormone laboratory, Department of Clinical Science

University of Bergen

June 2020

List of contents

Acknowledgements

First of all, I would like to thank my supervisors Johan Fernø (main supervisor) and Martha Haugstøyl (co-supervisor). Johan Fernø has been a highly interested and engaged supervisor, the effort he put in facilitating the lab work and giving feedback on my work has been highly valuable. My co-supervisor Martha Haugstøyl has been excellent in providing technical training and giving feedback on my thesis. I would also like to thank PhD.candidate Kristina Strand for helping with the flow cytometry analyses, and lab technician Linn Skartvedt for providing assistance with the RNA isolation which has been highly appreciated. And I would like to thank Brith Bergum at the Flow Cytometry core facility for her technical guidance. I would also like to thank everyone at the research group at the Hormone laboratory who have contributed with advice and support during my thesis.

I would like to thank Karin Stenkula and Claes Fryklund from Lund university for their contribution at Voss hospital. Their insight and technical knowledge were essential for the experiment. I would also like to thank the staff at Voss hospital for their hospitality and for facilitating our lab work. And I like to thank all the patients which has participated in this study, their willingness to contribute is absolute essential.

I would also like to thank Silvana Hengler from Hohenheim university for her assistance at the lab and the insight she supplied in R-programming.

My girlfriend, Andrea Bjerketvedt has been a fantastic support

Bergen, June 2020

Eirik Nordahl-Pedersen

Abbreviations

AKT – Ak strain transforming/Protein kinase B

AMPK – AMP activated protein kinase

AT – Adipose tissue

ATM – Adipose tissue macrophages

BAT – Brown adipose tissue

BMI – Body mass index

CVD – Cardiovascular disease

DAG – Diacylglycerol

ECM – Extra cellular matrix

FFA – Free fatty acids

GLUT4 – Glucose transporter 4

HFD – High fat diet

IKK-β – Inhibitor of nuclear factor kappa-B kinase subunit beta

IRS-1 – Insulin receptor substrate 1

JNK – c-Jun N-terminal kinases

MHO – Metabolically healthy obese

MUH – Metabolically unhealthy obese

NF-κB – Nuclear factor kappa B

PBMC – Peripheral blood mononuclear cells

PDK1 – Phosphoinositide-dependent protein kinase-1

PI3K – Phosphatidylinositol-3-kinase

PIP2 – Phosphatidylinositol 4,5-

PIP3 – Phosphatidylinositol-3,4,5-triphosphate

PKC – Protein kinase C

PPAR – Peroxisome proliferator-activated receptor

RBC – Red blood cells

SAT – Subcutaneous adipose tissue

SVF – Stromal vascular fraction

T2DM – Type 2 diabetes mellitus

TLR4 – Toll-like receptor 4

VAT – Visceral adipose Tissue

WAT – White adipose tissue

Summary

The prevalence of obesity has increased substantially in the recent decades, along with associated co-morbidities such as insulin resistance, type 2 diabetes mellitus (T2DM) and cardiovascular diseases (CVDs). Moreover, obesity is associated with a state of chronic low-grade inflammation which is thought to be one of the main driving forces for the development of insulin resistance and T2DM. However, the causal relationship is still controversial. The inflammation in adipose tissue has been characterized by the secretion of pro-inflammatory cytokines and infiltration of pro-inflammatory macrophages. In particular, an increased tendency of accumulating fat in the visceral adipose tissue have been associated with adipose tissue inflammation and an increased risk of associated co-morbidities.

In this project, we aimed to quantify the level of macrophage infiltration into subcutaneous (SAT) and visceral adipose tissue (VAT) of severely obese subjects undergoing bariatric surgery. Furthermore, we phenotypically characterized pro-inflammatory M1-like macrophages (CD11c+CD206+) and anti-inflammatory M2-like macrophages (CD11c-CD206+) by the expression of known pro-inflammatory receptors and investigated whether the level of pro- and anti-inflammatory macrophages associated with insulin resistance and other clinical parameters relevant for metabolic syndrome. We also analyzed the expression level of pro- and anti-inflammatory genes and performed functional analysis on isolated mature adipocytes from SAT and VAT, focusing on differences between the two depots.

We found that macrophages are more abundant in SAT than in VAT. Moreover, insulin resistance (HOMA-IR) was associated with a higher ratio of the anti-inflammatory M2/M1-like macrophages and a higher expression of the anti-inflammatory receptors CD163 and TREM2 in SAT. We also found that systemic inflammation was associated with a higher ratio of pro-inflammatory M1/M2-like macrophages and a pro-inflammatory gene expression pattern in VAT. Moreover, the chemotactic receptor, CCR2, was found to be highly expressed by M1-like macrophages and almost absent from M2-like macrophages. Further, we found that lipolysis was significantly higher in VAT compared to SAT of obese subjects, and the lipolytic response correlated negatively with insulin sensitivity in VAT.

1. Introduction

1.1 Obesity

Obesity is a complex disease and a major public health concern because of its increasing prevalence worldwide. Obesity results from excessive caloric intake over time. Excessive calories in the form of carbohydrate, fat and proteins are converted into triglycerides which are stored in adipose tissue leading to expanding adipose tissue (Burhans, Hagman et al. 2018). A common method to quantify the level of obesity have been the BMI (body-mass index) scale, where the weight in kilograms is divided by the square of the height in meters (Chooi, Ding et al. 2019). A BMI of 20-25 defines the normal healthy level, 25-29 as overweight and above 30 as obesity, while above 40 is considered morbidly obese. However, using the BMI designation to quantify obesity is limited by the fact that it cannot distinguish between fat and muscle mass and is not diagnostic of the body fatness, health status and associated risks. Furthermore, BMI do not differentiate between different fat depots (Chooi, Ding et al. 2019).

Obesity is associated with elevated risk of several severe implications, such as metabolic syndrome, insulin resistance and T2D, atherosclerosis and an elevated risk of several forms of cancer which has brought a lot of attention in research on the pathogenesis of obesity (Apovian 2016).

1.2 Epidemiology

The prevalence of obesity has increased substantially in the last four decades and, nearly a third of the world population is now classified as overweight or obese. If the current trend continues it is estimated that more than half of the world population will be overweight or obese by 2030 (Chooi, Ding et al. 2019). Obesity is considered a major risk factor for developing insulin resistance and T2DM. Studies show that about 80% of the individuals diagnosed with T2DM are obese (Kennedy, Martinez et al. 2009). Besides increasing the risk of several serious diseases, obesity has a major socioeconomic cost by impacting on quality of life, work productivity and health costs. The cause of the obesity epidemic has been

attributed to the modern western diet consisting of more processed, energy dense, nutrient poor and affordable food and beverages which facilitates overconsumption. A major contribution also comes from a coincidence of decreased physical activity in the population owing to modernization of lifestyles (Chooi, Ding et al. 2019). In high income countries, obesity is most prevalent among poor and disadvantaged groups at all ages, while in low income countries obesity mostly affect middle-aged people from wealthy and urban environments. Also, the prevalence of obesity is generally higher in women than men at all sociodemographic levels (Chooi, Ding et al. 2019). During the last decade or so it has been observed that the increase in obesity rates have levelled off to some extent in many of the high-income countries. On the other hand, the obesity rates have accelerated in other parts of the world, especially in developing countries. This is most likely a result of rapid change in socioeconomic status, and adaption of a western diet accompanied by a more sedentary lifestyle, but globally the rate is still increasing (Chooi, Ding et al. 2019). It is debated whether the obesity epidemic may be slowing down in Norway as well. But a large study in the adult population in Norway (n = 90000) found that from the period 1984-1986 through 1995-1997 to 2006-2008 the mean BMI increased from 25.3 to 26.5 and 27.5 kg/m^2 in men and from 25.1 to 26.2 and 26.9 kg/m^2 in women respectively. While the increase in prevalence of obesity (BMI >30 kg/m2) raised from 7.7 to 14.4 and 22.1% for men and from 13.3 to 18.3 and 23.1% in women during the same period and found no signs of reduction in incidence of obesity during the follow-up period (Midthjell, Lee et al. 2013). Concomitant with the increase in obesity there have been a rapidly increase in incidence and prevalence of T2DM. A large metanalysis of 751 studies including 4 372 000 adults from 146 countries found that the global prevalence increased from 4.3% in 1980 and up to 9% in 2014 for men and from 5.0% up to 7.9% for women (Collaboration 2016). The number of total diabetes cases raised from 108 million up to 422 million during the same period. Lowest prevalence was observed in northwestern Europe and highest prevalence was observed in Polynesia and Micronesia (Collaboration 2016). In Norway, the incidence rate has been reported to level off to some degree in recent years. From 2009 to 2014 it was reported that the incidence decreased from 609 cases per 100 000 persons a year down to 398 cases per 100 000 persons a year in 2014. Meanwhile the prevalence is still increasing, up from 4.9% to 6.1% during the same period, and is probably explained by diagnosis at a younger age and increased longevity (Ruiz, Stene et al. 2018).

1.3 Insulin resistance and Type II diabetes

Because of the increasing prevalence of T2DM worldwide, it has been put down a lot of effort to understand the mechanisms of insulin resistance and β-cell dysfunction which are the leading cause of T2DM (Kahn, Cooper et al. 2014). In the normal healthy state, glucose metabolism is regulated by a feedback loop involving the insulin secreting islet β-cell of the pancreas and insulin sensitive tissue such as liver, muscle, and adipose tissue (Kahn, Cooper et al. 2014). Insulin is secreted in response to elevated blood glucose levels in the postprandial phase and acts by suppressing glucose production in the liver and stimulates uptake of glucose in liver, muscle and adipose tissue by promoting translocation of GLUT4 to the plasma membrane (Kahn, Cooper et al. 2014). Most of insulin action is mediated by AKT which is activated in a signaling cascade downstream of the insulin receptor (Figure 1.1.A). AKT also stimulates anabolic processes such as glycogenesis, de novo lipogenesis and protein synthesis, while at the same time inhibiting the opposing pathways (Huang, Liu et al. 2018). Perturbation of components in the insulin signaling cascade is a characteristic of insulin resistance and consequently lack of AKT stimulation diminishes GLUT4 translocation to the membrane leading to elevated blood glucose levels, which is magnified by the lack of inhibition of gluconeogenesis in liver (Figure 1.1. B). Lack of AKT signaling also diminishes the inhibitory effect on lipolysis, increasing the levels of circulating free fatty acids (FFA) which is taken up by muscles, liver and pancreas or deposited on ectopic places, contributing to lipotoxicity (Huang, Liu et al. 2018). It has been found that FFA and other metabolites that are increased during insulin resistance such as diacylglycerol (DAG), ceramides and acyl-CoA, could stimulate several protein kinases such as IKK-β, JNK and several isoforms of PKC to phosphorylate IRS-1 (Figure 1.1.B) attenuating the insulin signaling pathway (Szymczak-Pajor and Sliwinska 2019).

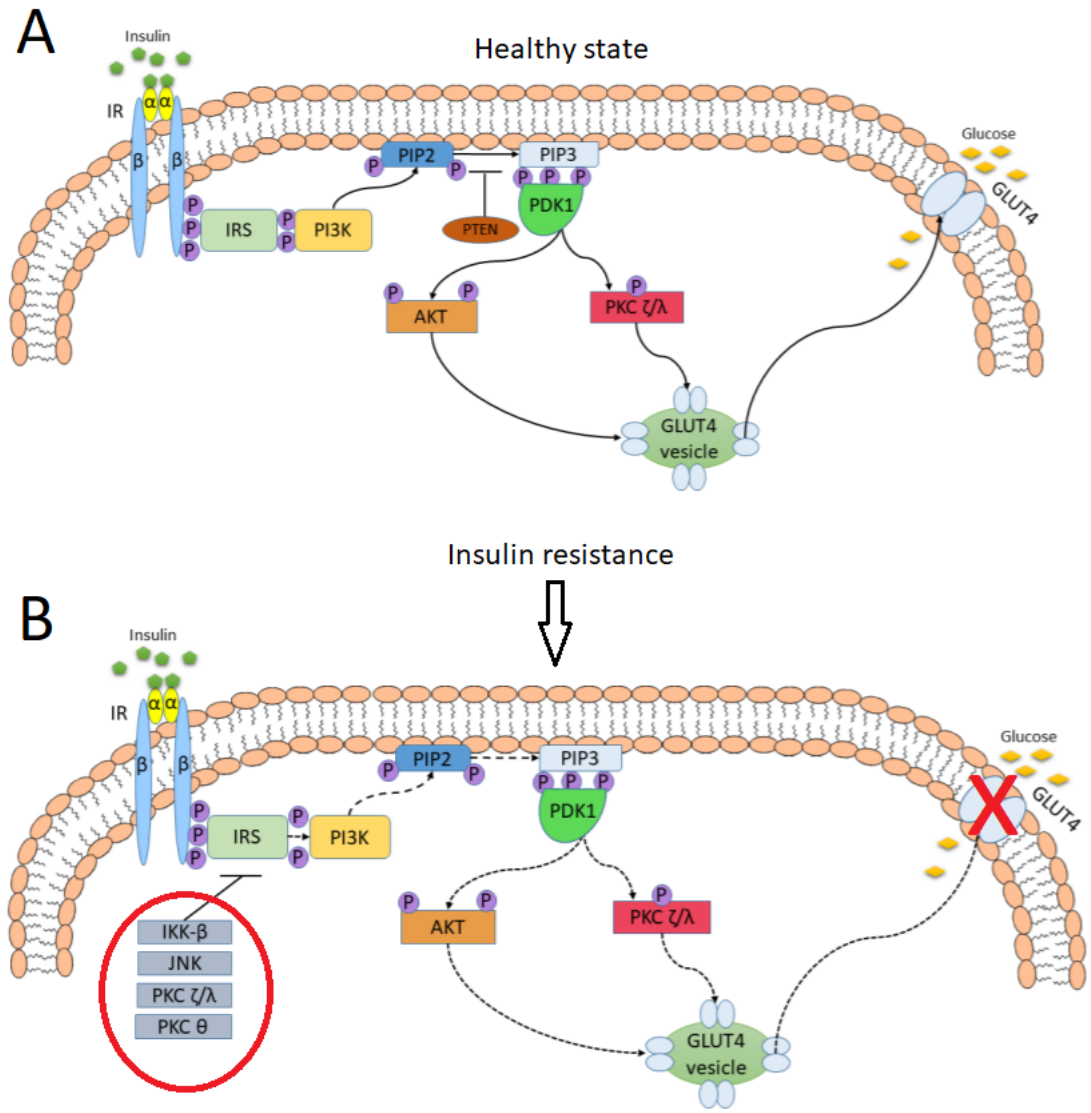

Figure 1.1 The insulin signaling pathway during normal physiological conditions (A) and insulin resistance (B). *Insulin binding to its receptor is followed by dimerization and autophosphorylation of tyrosine residues on the cytosolic part of the receptor. Phosphotyrosine functions as docking sites for insulin-receptor substrate proteins which gets phosphorylated by the receptor and promote activation and translocation of PI3K to the membrane were PI3K phosphorylates PIP2 to PIP3. Elevation of PIP3 promotes activation of serine threonine kinase PDK1, which phosphorylates PKC and AKT leading to their activation. AKT and PKC mediates translocation of glucose transporters GLUT4 to the plasma membrane to elevate glucose uptake. AKT also promote glycogenesis, lipogenesis and protein synthesis. During insulin resistance (B), the insulin signaling pathway is attenuated by inhibitory phosphorylation of IRS1 by several kinases such as IKK-β, JNK, and different isoforms of PKC. Failure of translocating GLUT4 to the plasma membrane leads to elevated blood glucose, in addition AKT will not mediates its other actions in response to insulin such as inhibiting lipolysis and gluconeogenesis in adipose tissue and liver, respectively (Szymczak-Pajor and Sliwinska 2019).*

The amount of insulin secreted from the β-cells are dependent upon the sensitivity of the target tissue, and when insulin resistance develops the β-cells try to cope with that by increasing insulin secretion to maintain glucose homoeostasis. Impaired glucose tolerance recognized by prolonged elevated glucose levels after a meal arise when the β-cells are incapable of increasing insulin secretion to cope with the worsening insulin resistance eventually leading to β-cell dysfunction (Kahn, Cooper et al. 2014). T2DM is a heterogeneous disease characterized by β-cell dysfunction in the pancreas, affecting insulin secretion and the insulin sensitivity in target tissues. The causes include both genetic and environmental contributions (Kahn, Cooper et al. 2014). Obese individuals are found to have a higher risk of developing T2DM suggesting that adipose tissue is likely to play a role in the pathogenesis of the disease (Scheen 2003). The level of insulin resistance has commonly been quantified by the HOMA-IR scale, which is calculated on the fasting levels of glucose and insulin (equation 1.1) (Kim, Seol et al. 2019).

(1.1)

$$HOMA - IR = \frac{Glucose\ \left(\frac{nmol}{L}\right) * Insulin\ \left(\frac{\mu U}{mL}\right)}{22{,}5}$$

1.4 Adipocytes and adipose tissue

Adipose tissue serves several important physiological functions in our body and is commonly divided into two subtypes, white adipose tissue (WAT) and brown adipose tissue (BAT) (Saely, Geiger et al. 2012). WAT is most abundant and could broadly be divided into subcutaneous adipose tissue (SAT) which is located underneath the skin, and the visceral adipose tissue which surrounds the internal organs. The main role of WAT is to store excess calories consumed in the form of triglycerides, which can be used later for energy (Murawska-Cialowicz 2017). WAT also serves an important function as an endocrine organ, secreting adipokines, such as leptin, adiponectin and omentin which have important regulatory functions on fatty-acid oxidation, lipogenesis, gluconeogenesis, glucose uptake and insulin signaling in metabolically important tissues such as skeletal muscle, liver and

brain (Chait and den Hartigh 2020). BAT serves a function in heat production by metabolizing fatty acids and dissipates the energy as heat through mitochondrial uncoupling. BAT is most abundant in newborns and in particular small mammals enabling them to thrive in cold environments. The extent of BAT in adults and its physiological relevance is still not fully elucidated (Saely, Geiger et al. 2012). WAT is composed mostly of adipocytes, loose connective tissue and the stromal vascular fraction (SVF), which includes fibroblasts, preadipocytes, vascular endothelial cells and immune cells such as macrophages, NK-cells, T- and B-lymphocytes (Martyniak and Masternak 2017). WAT exhibits a tremendous capacity of expansion, mostly through the process of cell growth known as hypertrophy, but also through division of stem cells and differentiation of pre-adipocytes, a process known as hyperplasia (Zhang, Xie et al. 2017). Several studies have shown that there are great inter-individual differences in the capacities of hypertrophy and hyperplasia, which could have implications for disease risk (Zhang, Xie et al. 2017).

1.5 Adipose tissue depots and metabolically healthy obesity

Some obese individuals appear to be better protected against metabolic abnormalities and has been referred to as metabolic healthy obese (MHO) (Iacobini, Pugliese et al. 2019). It is widely accepted among researchers in the field that central body fat distribution and impaired adipose tissue function are better predictors of obesity-associated metabolic syndrome than total fat mass and BMI (Iacobini, Pugliese et al. 2019). To eliminate subjective bias, it has been suggested that six parameters should be considered in classifying metabolic syndrome: waist circumference, insulin resistance, blood sugar levels, blood pressure, cholesterol levels and physical fitness. Which parameters best defining MHO has not been established yet, but most researchers agree on reduced accumulation of visceral adipose tissue (VAT) and ectopic fat, preserved insulin sensitivity and a lower degree of systemic and adipose tissue inflammation to be some of the defining features of MHO (Iacobini, Pugliese et al. 2019).

Several factors regulate fat distribution in various adipose tissue depots. Age, sex and total body fat content are the main predictors of body fat distribution, but evidence indicates that genetic factors also have a major impact on fat distribution at any given BMI. Several studies

have attested the waist to hip ratio, a measure of fat distribution and found it to be highly heritable with estimates of up to 60% (Goodarzi 2018). SHOX2 is an example of a gene pointed out as a major determinant of regional fat distribution. SHOX2 expression in subcutaneous adipose tissue (SAT) correlates positively with both lipolysis activity of SAT adipocytes and visceral adiposity (2016). Also, there is evidence that developmental genes are differentially expressed in various fat depots and might play a role in the regulation of fat distribution and thereby also obesity-related metabolic traits (2016). This suggest that the difference between the MHO and metabolically unhealthy obese (MUO) phenotype is partly caused by genetic traits modulating body fat distribution between the different fat depots, which hold diverse biological properties and functions. Evidence indicates that not all fat depots are equally hazardous for health. Stronger associations are found between VAT and ectopic fat accumulation around liver, heart and muscles, with insulin resistance and CVD (Lebovitz and Banerji 2005). The type of fat also matters, WAT is strongly associated with obesity related metabolic disorders. BAT, on the other hand has a large potential of fat burning and confers a protective role for metabolic and cardiovascular health, although its contribution on whole body glucose homeostasis is still questionable (Chondronikola, Volpi et al. 2014).

MHO subjects are characterized by a greater tendency of storing fat in the SAT depot and less in VAT, and ectopic sites compared to MUO at the same BMI and fat mass. A greater tendency of fat accumulation in the lower part of the body compared to abdominal fat accumulation is also a determinant of MHO (Iacobini, Pugliese et al. 2019). Therefore, the reason why MHO are better protected against obesity related disorders could in part be explained by the divergent regulatory functions of VAT and SAT, contributing to a greater capacity of SAT expansion to buffer against lipid overflow, and thereby reducing fat deposition in abdominal VAT and at ectopic sites such as muscle, pancreas and liver (Iacobini, Pugliese et al. 2019). In summary, the metabolic health of an individual is likely to depend on the adipogenic capacity of adipose tissue, which favor lipid buffering. For each individual there is a threshold for the adipogenic capacity, and once this threshold is exceeded, lipids get deposited on ectopic sites leading to metabolic abnormalities (Iacobini, Pugliese et al. 2019). This hypothesis of a personal fat threshold could also explain the existence of metabolic unhealthy lean individuals. In addition, studies have found that

lifestyle habits might partly explain the heterogeneity of obesity in terms of metabolic abnormalities. In line with that, MHO phenotype is more frequently observed in younger and female adults, and in addition, the MHO is more likely to exercise and less likely to smoke or drink heavily (Iacobini, Pugliese et al. 2019).

1.6 Adipocyte cell size and insulin resistance

In order to maximize the amount of energy stored by each adipocyte, these cells are forming a large lipid droplet comprising almost the entire volume of the cell, only separated from the plasma membrane by a thin rim of cytoplasm (Zhang, Xie et al. 2017). During obesity the adipocytes increase their volume tremendously, and studies have found that adipocyte size has been correlated with obesity associated diseases such as T2DM and insulin resistance (Zhang, Xie et al. 2017). In line with this finding, obese subjects with a greater quantity of smaller adipocytes, indicative of a greater tendency of hyperplastic growth seems to be better protected against obesity related diseases (Zhang, Xie et al. 2017). In support to this, GWAS has found associations of genes involved in regulation of adipocyte development such as PPAR-γ with insulin resistance, and failure of adipocyte development as occurs in some lipodystrophy diseases causes severe systemic insulin resistance (Petersen and Shulman 2018). The orphan nuclear receptor NR4A1, also known as NUR77 is an important component in the regulatory control of adipocyte quiescence, and its expression is found to have a negative influence on the metabolically beneficial adipose tissue plasticity (Zhang, Federation et al. 2018). NR4A1 could thus be a major contributor to the tendency of mature adipose tissue to expand primarily through hypertrophic rather than hyperplastic growth and may account for some of the inter individual variability. It has been hypothesized that obesity represent a state with relative resemblance to lipodystrophy, and that T2DM arise when the adipocyte hypertrophic and hyperplastic capacity is insufficient to accommodate the metabolic stress of chronic caloric excess, leading to an increasing tendency towards lipids being deposited on ectopic places such as the liver, pancreas and muscle (Zhang, Federation et al. 2018).

1.7 Ectopic fat deposition, adipocyte lipolysis and insulin resistance

Adipocytes serve important functions during period of energy demand such as fasting or physical exercise by mobilizing fatty acids to serve as energy in tissues such as muscle, and to provide fatty acids and glycerol to the liver for synthesis of ketone bodies, and to serve as precursor for production of glucose in the process of gluconeogenesis respectively (Lass, Zimmermann et al. 2011). During lipolysis, triacylglycerols are hydrolyzed into fatty acids and glycerol by the sequential action of the three major lipases adipose triglyceride lipase (ATGL), hormone sensitive lipase (HSL) and monoacylglycerol lipase (MAGL). FFA and glycerol are released into the circulation and transported to tissues such as muscle and liver (Lass, Zimmermann et al. 2011).

Lipolysis is carefully regulated by the actions of catecholamines, natriuretic peptides and insulin. Catecholamines and natriuretic peptides are considered the main stimulators of lipolysis, although some catecholamines are inhibitory, while insulin is considered the main hormone for inhibition of lipolysis (Lass, Zimmermann et al. 2011). Studies have found that the lipolytic response of catecholamines is reduced in SAT but increased in VAT of obese and insulin resistant subjects (Lass, Zimmermann et al. 2011). Moreover, it is reported that the basal rate of lipolysis is increased in the obese state, which could be a consequence of the tremendous volumetric expansion of adipocytes in obesity to the point were further expansion is not feasible. It is hypothesized that the increased rate of basal lipolysis worsens the lipid accumulation on ectopic sites such as liver, pancreas and muscle, leading to impaired insulin sensitivity in those tissues (Lass, Zimmermann et al. 2011). In addition, higher rates of lipolysis may modulate the secretory profile of adipocytes to release adipokines and promote adipose tissue inflammation by stimulate resident adipose tissue macrophages (ATM) to production of cytokines and chemokines, attracting additional macrophages. Numerous studies have pointed on the association between ectopic lipid accumulation and insulin resistance. Ceramides and DAG is pointed out as the suspected molecular species impairing insulin signaling, and studies has shown that lipid infusion in healthy lean people transiently increase cytosolic DAG content and promote insulin resistance (Morigny, Houssier et al. 2016). Moreover, studies in rats has shown that DAG is

able to activate PKCε which directly interfere with the insulin signaling pathway by phosphorylating components in the pathway such as IRS1 and RPS6 (Gassaway, Petersen et al. 2018). It is also believed that the increase in circulating FFA and glycerol exacerbate hyperglycemia by serving as precursors and also stimulate gluconeogenesis (Morigny, Houssier et al. 2016). In addition, elevated FFA can acts as ligands for TLR4 receptors on macrophages, activating the NF-κB pathway leading to cytokine release (Kim, Seol et al. 2019).

1.8 Adipose tissue as an endocrine organ

Although adipose tissue traditionally has been recognized for its function in energy storage the latest decades of research have firmly elucidated its endocrine function. Already in 1987 it was discovered that adipose tissue has an important function in metabolism of sex hormones, and in 1994 followed the discovery of leptin, a hormone which have shown to play a major role in obesity (Mark 2013). It is now well established that adipose tissue secretes a wide variety of autocrine, paracrine and endocrine peptide hormones known as adipokines (Kershaw and Flier 2004). It is also found that adipose tissue expresses an array of receptors that enables the tissue to respond to signals from endocrine organs elsewhere in the body and the central nervous system. Through this network it is shown that adipose tissue is an important contributor in coordinating processes such as energy metabolism, neuroendocrine function and immune function (Kershaw and Flier 2004).

Leptin has been discovered as an adipokine with a central role in energy homeostasis which is mediated through hypothalamic signaling. Secreted leptin signals energy sufficiency by inducing sensation of satiety and contribute to reduced food intake and increased energy expenditure (Kershaw and Flier 2004). Leptin knock-out mice present with severe obesity which is shown to be reversed by leptin replacement. Nevertheless, many obese experience elevated levels of leptin and is resistant to the action of leptin, and thus cannot be treated by supplementing exogenous leptin (Kershaw and Flier 2004).

Adiponectin is another adipokine that is highly expressed and secreted by adipose tissue and accounts for 0.01% of total serum levels. Its expression is found to have a beneficial effect on insulin sensitivity, atherosclerosis and inflammation, and moreover, decreased expression of

adiponectin is closely associated with obesity (Chen, Montagnani et al. 2003). It is discovered that adiponectin has key roles in energy metabolism in several metabolically important tissues. Adiponectin is shown to activate AMPK, mediated through binding AdipoR1 receptor leading to increased insulin sensitivity and glucose uptake in adipose tissue, muscle and liver. In addition, adiponectin also inhibits gluconeogenesis in the liver by activating AMPK (Yilmaz, Biyikoglu et al. 2003), (Nawrocki, Rajala et al. 2006). Other actions of adiponectin are mediated through AdipoR2 receptors which activate the PPAR-α pathway leading to increased fatty acid oxidation and reduce inflammation (Kubota, Terauchi et al. 2002). The anti-inflammatory activity of adiponectin has implications for several inflammatory diseases including insulin resistance, atherosclerosis and cardiovascular diseases (CVDs). In vitro studies have shown that the anti-inflammatory actions of adiponectin are mainly driven by activation of AMPK and cAMP-PKA in macrophages, endothelial, epithelial and muscle cells, which stimulate the expression of anti-inflammatory IL-10. Moreover, in macrophages adiponectin also attenuates expression of the pro-inflammatory cytokines TNF and IL6 through inhibitory actions on the pro-inflammatory NF-kB pathway (Ouchi and Walsh 2007).

1.9 Adipose tissue as an immune organ and its implications for disease

Besides its roles in fat storage and endocrine functions, adipose tissue has also been recognized as an immune organ (Stolarczyk 2017). Adipose tissue hosts a vast array of immune cells such as macrophages, NK-cell, T- and B-lymphocytes. Research have discovered that composition of different immune cell populations is modulated in the setting of obesity, and obesity is now recognized as a low-grade chronic inflammatory disease (Stolarczyk 2017). In lean individuals, adipose tissue secretes anti-inflammatory adipokines such as IL-10 and resident immune cells exhibit an anti-inflammatory phenotype (Pahlavani, Ramalho et al. 2017). In obesity, it has been reported that secretion of IL-1β, TNF, IFN-γ and MCP-1 by adipocytes and resident immune cells attracts additional immune cells such as macrophages, NK-cells, T- and B-cells into the tissue and exacerbate the inflammation. (Stolarczyk 2017). Moreover, the proinflammatory cytokines TNF and IL6 have been shown to suppress the insulin signaling in adipocytes suggesting a causal link between inflammation

and insulin resistance (Stolarczyk 2017). The most prominent of the infiltrating immune cells are the macrophages which is found to account for 30-50% of the non-adipocyte cell fraction in adipose tissue (Boutens and Stienstra 2016). Although obesity is associated with a state of chronic low-grade adipose tissue inflammation, the immune cells that infiltrates adipose tissue during obesity also perform important homeostatic functions such as breaking down extracellular matrix (ECM) proteins to permit healthy expansion of adipose tissue by creating room for new adipocytes, followed by creation of new ECM, a process known as tissue remodeling. This process is mainly driven by macrophages which also stimulate angiogenesis, the development of new blood vessels to provide oxygen and nutrients to the expanding adipose tissue (Burhans, Hagman et al. 2018). Macrophages are also able to take up FFA that expanded adipocytes are unable to store. It has been discovered that macrophages gather around dying adipocytes, making up an aggregate which is described as crown-like structures, where macrophages contribute to clearance of lipids and removal of cellular debris. Through these mechanisms macrophages thereby provide an additional layer of lipid buffering capacity (Cinti, Mitchell et al. 2005).

More recent research has led to the hypothesis that adipose tissue in obesity transform from healthy expanding tissue into becoming inflamed when the ability of the tissue to induce adipogenesis and differentiate new adipocytes becomes limited. The continued exposure to excess nutrients leads to a stress response in enlarged adipocytes, causing them to express and secrete pro-inflammatory adipokines such as TNF-α, MCP-1 and IL6 which results in infiltration of bone-marrow derived monocytes and a polarization of macrophages into a pro-inflammatory state (Burhans, Hagman et al. 2018). It is proposed that the adipose tissue inflammation is part of a protective mechanism, by inducing insulin resistance to prevent cell death, and to provide additional lipid buffering capacity from the macrophages. During short-term caloric excess, low-level inflammation and adipose tissue macrophage (ATM) activation could be beneficial in the sense of providing enough time for the adipose tissue to expand. But in situations of chronic caloric excess, the non-resolving inflammation could be detrimental, and the continued insulin resistance would lead to elevated lipolysis, overwhelming the lipid buffering capacity of macrophages and contribute to ectopic lipid storage (Burhans, Hagman et al. 2018).

Traditionally, two populations of ATMs have been described. In lean individuals they mostly confine to an alternative activated M2-like phenotype characterized by increased expression of IL10 and arginase and has mostly been associated with homeostatic functions such as facilitating adipogenesis. Another ATM population which is increased in obesity shows characteristic of the classical activated M1 macrophages and are distinguished by their high expression of the integrin CD11c, and other markers of classical M1-macrophages such as IL6 and nitric oxide synthase (Wentworth, Naselli et al. 2010). The macrophages are highly plastic cells and are likely to respond and adapt to their environment, and a phenotypic switch from the M2-like macrophages towards a pro-inflammatory M1-like phenotype has been associated with insulin resistance. Moreover, studies in obese mice have shown that ablation of CD11c+ cells improves insulin sensitivity (Patsouris, Li et al. 2008).

Immunohistochemistry and flow cytometry have been the most commonly used methods to quantify ATMs, usually by antibodies against the surface receptors CD68, CD14 CD206 or CD11c (Morgan-Bathke, Harteneck et al. 2017). However, the two methods show poor correspondence, and the fact that there is no unifying concept on how to best characterize macrophages and other immune cells possess a challenge when comparing results from different studies in this field of research. Immunohistochemistry has good intra-individual reproducibility and the advantage of being able to quantify ATMs from preserved whole tissue samples but requires high amount of tissue and is time consuming. However, improvements in software assisted immunohistochemistry quantification has refined the procedure (Morgan-Bathke, Harteneck et al. 2017). Flow cytometry requires less tissue and can count millions of cells in a few minutes. In addition, flow cytometry permits the simultaneous use of multiple antibodies, providing additional cellular information in one experiment. However, this can be complicated by the extensive macrophage autofluorescence (Fay, Carll-White et al. 2018). Another big obstacle by using flow cytometry is that the individual cell populations within the adipose tissue have to be effectively isolated, intact while preserving cellular function (Hagman, Kuzma et al. 2012). The cell populations are usually liberated from the tissue by the use of one of two different enzymatic preparations; either collagenase alone or a combination of collagenase, liberases and other proteases (Hagman, Kuzma et al. 2012). It is reported that there are marked differences in cell yields, viability and surface antigen expression between the two methods,

which makes it difficult to compare results across studies (Pilgaard, Lund et al. 2008). Studies comparing the different methods have reported the use of collagenase alone as superior to the use of liberase or liberase collagenase mixtures with respect to cell yield and preservation of cell surface receptors, with an optimal digestion time of 60-75 minutes (Hagman, Kuzma et al. 2012).

1.10 Aim of this study

The introduction is aimed to give an overview of how the physiological aberrations caused by obesity can lead to inflammation in the adipose tissue and how this could be linked to development of insulin resistance and T2DM. Our hypothesis is that inflammation arise when the hyperplastic and hypertrophic capacity of adipose tissue is insufficient to accommodate to lipid burden caused by chronic caloric excess leading to increased lipolysis, ectopic lipid storage, inflammation and insulin resistance.

The main questions we want to assess in this study are:

- Does the macrophages polarization correlate with severity of obesity and insulin resistance?
- Could the alleged pro-inflammatory M1-like macrophages be characterized by the expression of other know pro-inflammatory receptors?
- Is the expression level of proinflammatory cytokines in adipose tissue correlated with insulin resistance or circulating markers of inflammation?
- What is the relative difference between the adipose tissue depots with respect to inflammation and insulin resistance?
- How is lipolysis and glucose uptake in isolated adipocytes associated with systemic measures of insulin resistance (HOMA-IR) and other markers of metabolic syndrome?

2. Materials

2.1 Antibodies

Name	Fluorochrome	Dilution	Supplier	Cat.nr
CD3	PE-Cy5	1:50	Biolegend	300410
CD11c	PE-Cy7	1:100	Biolegend	337215
CD14	BV605	1:100	Biolegend	301834
CD16	BV711	1:100	BD Biosciences	563127
CD19	PE-Cy5	1:100	Biolegend	302210
CD40	PE	1:25	Biolegend	313006
CD44	PE-CF594	1:200	BD Biosciences	562818
CD45	AF700	1:400	Biolegend	304024
CD56	PE-Cy5	1:50	Biolegend	304607
CD163	AF647	1:100	BD Biosciences	562669
CD192 (CCR2)	BV421	1:100	Biolegend	357209
CD206	BB515	1:200	BD Biosciences	564668
HLA-DR	APC-Cy7	1:400	Biolegend	307617

2.2 Biological samples

Tissue	Group	Source
Human blood and adipose tissue	Bariatric Surgery patients	Voss hospital
Human Blood and adipose tissue	Cholecystectomy	Voss hospital

2.3 Reagents and chemicals

Name	Supplier	Cat.no
Collagenase type 1	Life Technologies	171000017
Formaldehyde (2% v/v in PBS)	Sigma	P6148
LIVE/DEAD Fixable Aqua Dead Cell Stain Kit	Invitrogen	L349665
Lymphoprep	Stemcell Techonologies	7851
Glucose, D-[^{14}C(U)]	Perkin Elmer	NEC042X050UC
Insulin (Actrapid 100 IU/mL)	Novo Nordisk	
Isoprenaline (247.72 g/mol)	Sigma	I5627-5g
Ultima Gold MV	Perkin Elmer	6013159
Dinonyl phthalate, 97%	Acros Organics	408771000

2.4 Buffers

Krebs-Ringer phosphate buffer (KRP)	Kreps-Ringer Hepes buffer (KRH)	Dulbecco`s Phosphate Buffered saline (D-PBS, Sigma #D5652)	Fluorescence activated cell sorting buffer (FACS)
• 136 mM NaCl • 20 mM HEPES • 5 mM KCl • 5 mM $MgSO_4$ • 5 mM NaH_2PO_4 • 1 mM $CaCl_2$ • pH 7.4	• 120 mM NaCl • 30 mM HEPES • 10 mM $NaHCO_3$ • 4 mM KH_2PO_4 • 1 mM $MgSO_4$ • 1 mM $CaCl_2$ • 200 nM Adenosine • 1 % BSA (w/v) • pH 7.4	• 8 g/L NaCl • 1.15 g/L Na_2HPO_4 • 0.2 g/L KH_2PO_4 • 0.2 g/L KCl • pH 7.4	• D-PBS (Sigma • #D5652) • 2 % (v/v) fetal bovine serum (FBS) • 2 mM EDTA

2.5 Commercial kits

Name	Supplier	Cat.no
High-Capacity cDNA Reverse Transcription Kit	Applied Biosystems	4368814
Free Glycerol Reagent	Sigma-Aldrich	F6428
LightCycler 480 SYBR Green I Master	Roche	04887352001
RNA/Protein/DNA purification PLUS kit	Norgen Biotec Corp	47700

2.6 qPCR primers

Target	Forward primer	Reverse primer
CD68	CCACACAGGGGTCTTTGG	GATGAGAGGCAGCAAGATGG
CD163	GAAGATGCTGGCGTGACAT	GCTGCCTCCACCTCTAAGTC
IFN-γ	GAACTCTTTTCTTAGGCATTTTGAAG	CACTCTTTTGGATGCTCTGGT
IL6	ATAGGACTGGAGATGTCTGAGG	GCTTGTGGAGAAGGAGTTCATAG
IPO8	CGGATTATAGTCTCTGACCATGTG	TGTGTCACCATGTTCTTCAGG
MCP1	AGTCTCTGCCGCCCTTCT	GTGACTGGGGCATTGATTG
NR4A1	ACAGCTTGCTTGTCGATGTC	GGTTCTGCAGCTCCTCCAC
TNF	CAGCCTCTTCTCCTTCCTGAT	GCCAGAGGGCTGATTAGAGA
TREM1	AGTTACAGCCCAAAACATGC	CAGCCCCCACAAGAGAATTA
TREM2	ACAGAAGCCAGGGACACATC	CCTCCCATCATCTTCCTTCA

2.7 Instruments

Name	Supplier
Axiocam ERc 5s	Zeiss
Centrifuge 5810	Eppendorf
GeneAmp PCR System 9700	Applied Biosystems
Heraeus Fresco 21 Centrifuge	Thermo Scientific
Inkubator 1000	Heidolph
Light Cycler 480 Real-Time PCR	Roche
LSR Fortessa	BD Bioscience
Tri-Carb 4910 TR Liquid Scintillation Analyzer	PerkinElmer
Spectra Max Plus 384	Molecular Devices

2.8 Software

Name	Supplier	Identifier
FlowJo 10	Tree Star	https://www.flowjo.com
R	R core team	https://www.r-project.org

3. Methods

To address the aims of this study, we characterized ATMs by flow cytometry, performed gene expression analysis in adipose tissue (AT), and measured glucose uptake and lipolysis in isolated mature adipocytes from SAT and VAT. The workflow in this study is illustrated in Figure 3.1.

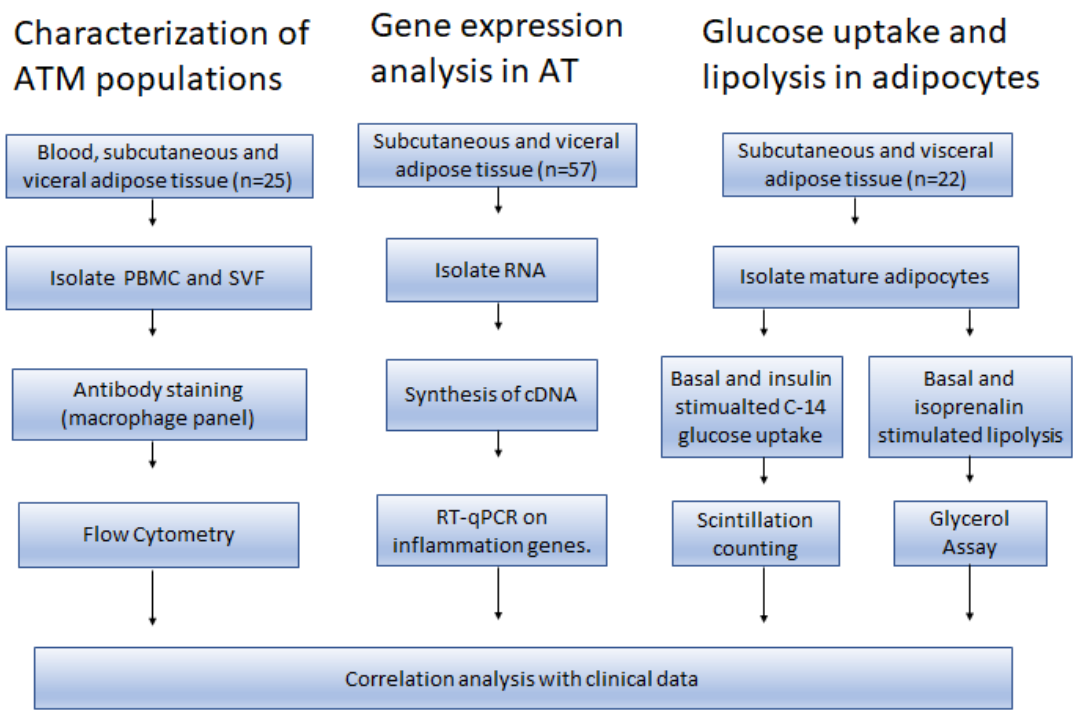

***Figure 3.1: Flowchart depicting the main steps of this project**. The project is divided in three main branches: gene expression analysis by qPCR, characterization of ATM by flow cytometry and glucose and lipolysis assay. Each branch includes a separate cohort of patients. Ultimately the data was subject for statistical analysis in R.*

3.1 Subjects

The study includes subjects from three different cohorts. The first cohort of subjects includes 57 morbidly obese patients undergoing bariatric surgery at Voss Hospital. SAT and VAT biopsies from this cohort was used for gene expression analysis. The second cohort was included in the flow cytometry analysis and comprise blood, SAT and VAT from 25 patients, 21 of which were morbidly obese and underwent bariatric surgery and 4 lean controls who

underwent cholecystectomy. The last cohort consists of SAT and VAT from 22 morbidly obese bariatric surgery patients at Voss hospital and was included in the glucose uptake and lipolysis experiments.

Gene expression analysis

3.2 Isolation of RNA

The adipose tissue was stored at -80°C freezer immediately after surgery and until usage. Total RNA was isolated from approximately 100 mg adipose tissue from the subcutaneous and visceral depot using the RNA/Protein/DNA purification kit. This work was done by a technician in our group.

3.3 Validation of input RNA in cDNA synthesis

An initial experiment resulted in high Ct values in the qPCR for some of the genes, and an additional experiment was therefore performed in order to validate the efficiency of the cDNA synthesis and find the best suitable concentration of cDNA to use in the RT-qPCR reactions. Two samples were selected, and for each sample three reactions were run with 100, 350 and 1000 ng of input RNA diluted in PCR grade water to give a total volume of 14.2 µL. A master mix was made using the High-Capacity Reverse Transcription Kit composed of 2 µL 10x RT Buffer, 0.8 µl 25x dNTP mix (100 mM), 2.0 µL 10x RT Random Primers and 1.0 µL Multiscribe Reverse Transcriptase. The RNA was added to the master mix to a total volume of 20 µL for each of the samples, and the reaction was run at the thermal cycler GeneAmp PCR System 9700 using the thermal cycling program listed in Table 3.1.

Table 3.1: *Thermal cycling program for cDNA synthesis.*

Time	Temperature
10 minutes	25°C
120 minutes	37°C
5 minutes	85°C
>5minutes	4°C

The cDNA was diluted 1:2 in PCR-grade water and qPCR was performed on selected genes, each sample run in triplicate according to Table 3.2. qPCR was run on Light Cycler 480 Real-Time PCR using the thermal cycling program listed in Table 3.3.
Based on this experiment, 350 ng of input RNA and a 1:2 dilution of the resulting cDNA was applied for the qPCR on all the target genes including reference gene.

3.4 qPCR

RT-qPCR was performed to quantify the relative expression of target genes. IPO8 was used as a reference gene in order to normalize for differences in input mRNA among samples. IPO8 is a nuclear protein involved in import of proteins into the nucleus through the nuclear pore complex (NPC) and studies have found it among the most stably expressed genes in both SAT and VAT (Hurtado del Pozo, Calvo et al. 2010). Sequence of the reference and target genes primers can be found in Table 2.6. A reaction master mix was made, composed of 1740 µL SYBR GREEN Master reagent, 174 µL (20 µM) each of forward and reverse primer, and 957 µL PCR grade water. Then a mix was made for triplicates of each cDNA sample, containing 24,5 µL of the mastermix and 3,5 µL of cDNA. The mix was transferred to a 384-well plate, 8 µL of each sample in triplicates. qPCR was run on Light Cycler 480 Real-Time PCR using the thermal cycling program listed in Table 3.3. The average expression levels for each triplicate was calculated relative to the expression of IPO8. Then the ΔΔCt-approach was used to calculate the fold change in expression level using the mean of all SAT samples as normalizer.

Table 3.2: Reaction mix for qPCR

Reagent	Volume (µL) per sample
Forward primer	0.4
Reverse Primer	0.4
SYBR GREEN master	4
PCR-grade water	2.2
cDNA	1

Table 3.3: *The thermal cycling program used in qPCR reactions consist of one pre-denaturation step and 45 cycles of denaturation, annealing and extension.*

		Time	Temperature
	Pre-denaturation	**5 minutes**	95°C
45 Cycles	**Denaturation**	**10 seconds**	95°C
	Annealing	**20 seconds**	60°C
	Extension	**30 seconds**	72°C

3.5 Isolation of PBMC from blood samples

Blood was collected in heparin tubes and stored overnight at room temperature (RT). 15 mL of blood was diluted 1:1 in PBS then carefully layered on top of 15 mL Lymphoprep and centrifuged (25 min, 2000 rpm) to separate PBMC from plasma and red blood cells. The layer containing PBMC was isolated and washed by adding 45 mL PBS and centrifuged (6 minutes, 1800 rpm), followed by staining for flow cytometry.

3.6 Isolation of stromal vascular cells from adipose tissue biopsies

Adipose tissue biopsies from SAT and VAT collected at Voss hospital were transported to our lab in 20 mL KRP buffer. Most of the biopsies were further processed after an overnight incubation at 4°C, while some were processed the same day. Larger blood vessels were excised from the biopsies and the remaining tissue cut into small pieces before enzymatic digestion with 0.66 mg/mL collagenase type I for 1 hour with shaking at 37°C. The tissue was filtered through 100 µm filters to remove connective tissue. The stromal vascular fraction was then isolated from the floating layer containing mature adipocytes, washed in PBS and centrifuged (5 minutes, 300g) before resuspending the pellet in PBS, followed by staining for flow cytometry.

Flow cytometric analysis

3.7 Compensation

Compensation controls were performed because of overlap in the emission spectra between several of the fluorochromes in the panel illustrated in Figure 3.2. For compensation, three drops of BD TM CompBeads containing Anti-Mouse Ig kappa and negative control beads were vortexed and mixed with 1.2 mL FACS buffer. Then, 50 µl of the beads was transferred into a 96-well plate and mixed with 0.5 µL of each of the antibodies listed in Table 2.1. Followed by a 20 minutes incubation in the dark at RT, the beads were washed twice with FACS buffer and centrifuged (3 minutes, 1600 rpm). Lastly, the beads were resuspended in 200 µL FACS buffer and run on 18-color LSR Fortessa equipped with 407, 488, 561 and 640 nm lasers. The compensation matrix was calculated in FlowJo 10.6.2 and adjusted manually.

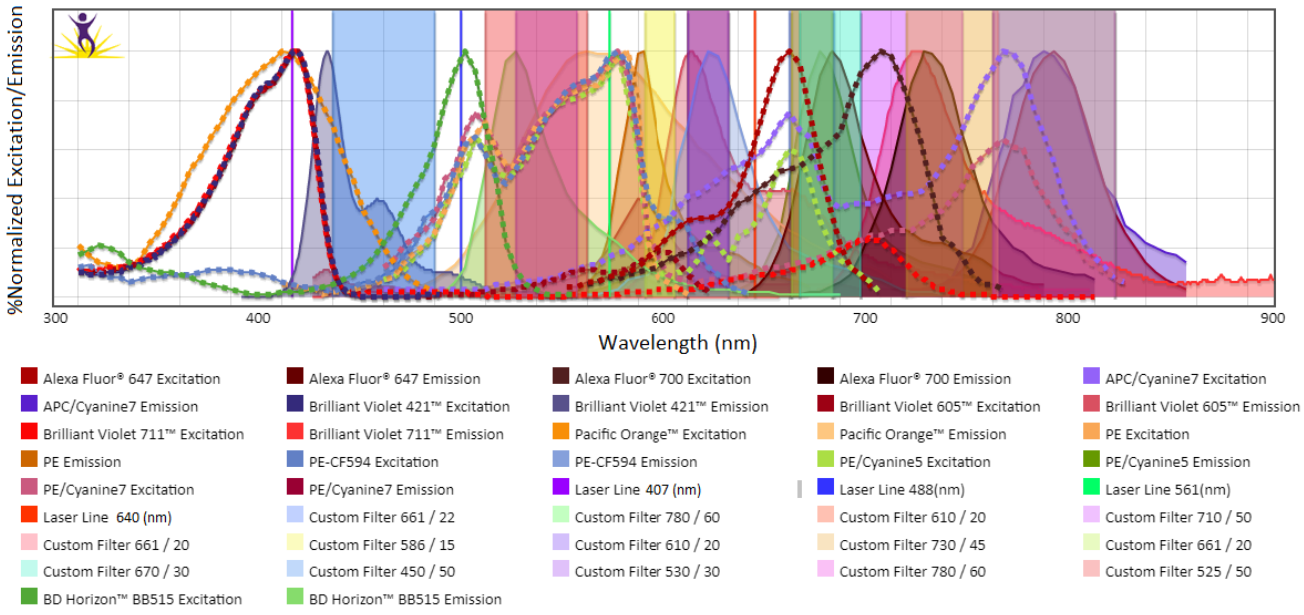

Figure 4.2. ***Spectral analysis of the flow cytometry panel (Biolegend).*** *Spectral analysis of the 12-color panel used in the staining of PBMC and SVF from SAT and VAT. Excitation (dotted line), emission (line), laser (vertical line) and filter (vertical band) are indicated.*

Table 4.4*: Overview of the Macrophage panel used in staining for flow cytometry. Antibody targets and dead cell marker, fluorochromes, dilution factors, wavelength for excitation and filters used for detection are listed.*

Antibodies/marker	Fluorochrome	Dilution	Excitation(nm)	Filter/bandpass(nm)
CD3	PE-Cy5	1:50	561	661/20
CD11c	PE-Cy7	1:100	561	780/60
CD14	BV605	1:100	405	610/20
CD16	BV711	1:100	405	710/50
CD19	PE-Cy5	1:100	561	661/20
CD40	PE	1:25	561	586/15
CD44	PE-CF594	1:200	561	610/20
CD45	AF700	1:400	639	730/45
CD56	PE-Cy5	1:50	561	661/20
CD163	AF647	1:100	639	670/30
CD192 (CCR2)	BV421	1:100	405	450/50
CD206	BB515	1:200	488	530/30
HLA-DR	APC-Cy7	1:400	639	780/60
DCM aqua	Pacific Orange	1:100	405	525/50

3.8 Staining of PBMC and SVF for flow cytometry

Freshly isolated PBMC and SVF were counted under the microscope using Burker counting chamber, and three million cells from each sample were added to a 96-well plate for centrifugation (3 min, 1600 rpm). The cells were resuspended in 50 µL of the master mix, containing antibodies, dead cell marker Aqua-Pacific Orange and FACS buffer, as listed in Table 3.5. The cells were incubated in 20 minutes in the dark at RT, followed by washing twice in FACS buffer (150 & 200 µL), and centrifuged (3 min, 1600 rpm). In addition, 2 million cells from selected PBMC sample were applied as unstained negative control. The cells were fixated in 2% formaldehyde (v/v in PBS) for 15 minutes in the dark at RT followed by washing twice in FACS buffer and centrifuged (3 min, 1600 rpm). Lastly, the cells were resuspended in 200 µL FACS buffer and applied on LSR Fortessa. The flow cytometry data was analyzed using FlowJo version 10.6.2.

Table 3.5: *Volume of Antibodies and dead cell marker used for staining of PBMC and SVF for each sample, FACS buffer was added to a total volume of 50 µL.*

Antibodies/marker	Volume (µL)
CD3	1.00
CD11c	0.50
CD14	0.50
CD16	0.50
CD19	0.50
CD40	2.00
CD44	0.25
CD45	0.13
CD56	1.00
CD163	0.50
CD192 (CCR2)	0.50
CD206	0.25
HLA-DR	0.13
DCM aqua	0.50
FACS buffer	41.80
Total	50.00

3.9 Gating strategy for quantification of macrophages

Gating was performed using FlowJo version 10.6.2. First, time versus forward scatter area was plotted, and a gate was drawn in order to exclude electronic noise. Then, forward scatter area was plotted against forward scatter height to gate for singlet cells, followed by gating for lymphocytes and monocytes/macrophages by plotting side scatter area against forward scatter area. Next, viable CD45 positive cells was gated for by plotting CD45 against the dead cell marker DCM-aqua. Then, a dump channel was applied by plotting CD11c against CD3, CD19 and CD56, and a gate was drawn to exclude the CD56, CD19 and CD3 positive NK-cell, B- and T- lymphocytes respectively. Lastly, side scatter area was plotted against HLA-DR in order to gate for the HLA-DR positive macrophages and monocytes. The fraction of macrophages was normalized to total of CD45 positive viable cells. To calculate fraction of M1-, M2-like macrophages and monocytes of the total macrophage count, CD206 was plotted against CD11c and the subpopulations were defined as monocytes (CD11c+

CD206-), M1-like macrophages (CD11c+ CD206+) and M2-like macrophages (CD11c- CD206+). For each subpopulation, the fraction of CCR2, CD16 and CD163 expressing cells was calculated by plotting side scatter area against CCR2, CD16 and CD163, respectively and a gate was drawn on cells positive for the respective markers (supplementary Figure 1). The expression of CD14, CD40, CD44 and HLA-DR was calculated by applying the geometric mean function in FlowJo and results presented as log mean fluorescence intensity.

Glucose uptake and lipolysis

3.10 Isolation of mature adipocytes

Subcutaneous and visceral adipose tissue biopsies arrived directly from surgery in 20 mL KRP buffer. First, the biopsies were cut clean of larger blood vessels and connective tissue, followed by weighing in from 1-1.5 gram of adipose tissue. The tissue was succumbed in 5 mL of prewarmed (37°C) KRH buffer and cut into small pieces. Then, the tissue was incubated in 1 mg/mL collagenase I for 30-40 minutes at 37°C and shaking at 214 rpm. Followed by digestion, 5 mL of KRH buffer was added to dilute the enzyme, and the tissue was filtered through 400 µm filters and placed in 37°C water bath for 5 minutes to let the adipocytes separate from the SVF by floatation. The bottom layer, containing the SVF, was removed with a syringe and the adipocytes washed in 5 mL KRH buffer twice followed by incubation for 50-60 minutes at 37°C water bath to let the mature adipocyte float and pack densely as a top layer. Lastly, the KRH buffer was removed and the isolated adipocytes were diluted in KRH buffer to a 7.5% cell suspension.

3.11 Glucose uptake

The cell suspension was placed on a magnetic stirrer to ensure a homogenous suspension, and 200 µl of the cell suspension was transferred, and added 200 µL insulin diluted in KRH buffer to a final concentration of 10 nM. To measure basal glucose uptake, 200 µL of the cell suspension was added equal amount of KRH buffer. After 30 minutes of incubation at 37°C with shaking, 100 µL (9,25 kBq/mL) of C-14 glucose was added and incubated for another 30 minutes. Lastly, 300 µL of the cell suspension was layered on top of Dionyl phthalate and centrifuged 1 minute at 12000 rpm to separate the cells from the medium. The samples

were then frozen at -20°C and transported to the Hormone laboratory in Bergen for further analyses. The first samples from the first 13 patients were run in duplicates, while the last nine were run in triplicates.

3.12 Scintillation counting

The separation of cells resulted in three distinct layers, with the cells at the top separated from the medium by the oil layer in the middle composed of Dionyl phtalate. The tubes were taken directly from -20°C freezer and cut in two. The upper part containing the cells were transferred to a 25 mL scintillation tube together with 15 mL of Ultima Gold scintillation fluid. The disintegrations from the C-14 glucose taken up by the cells was then counted in PerkinElmer Tri-Carb 4910 TR Liquid Scintillation Analyzer at 5 minutes with 1-minute pre-count delay.

3.13 Lipolysis assay

For the first six patients samples the cell suspension was diluted to 3.75%, and for the seventh patient onward a 7.5% cell suspension was used. To measure both stimulated and basal lipolysis, 400 µL of the cell suspension was incubated both with and without 10 nM of the β-adrenoreceptor agonist, isoprenaline, for 30 minutes at 37°C while shaking. The cell suspension was then placed on ice for 30 minutes to stop the assay and let the adipocytes float. 160 µL of the glycerol containing medium was then transferred by a thin pipette and frozen at -20°C until further analyses. All samples were run in duplicates.

3.14 Glycerol detection assay

In periods of energy demands, adipocytes mobilize their fat store by hydrolytic cleavage of TAGs, releasing non-esterified fatty acids and glycerol into the circulation in a 3:1 stoichiometry (Lass, Zimmermann et al. 2011). To quantify the lipolysis, we measured glycerol released from the cells into the medium using the Free Glycerol detection Reagent (Sigma Aldrich). The Glycerol Reagent generates a quinoneimine dye using coupled enzyme

reactions. The dye shows an absorbance maximum at 540 nm and the absorbance is directly proportional to the free glycerol concentration of the sample.

For each of the samples from the lipolysis assay, 30 µL was mixed with 100 µL Free Glycerol reagent and incubated for 15 minutes in dark at RT, in addition to a dilution series of 0.125, 0.25, 0.50, 1.00, and 2.00 mM glycerol in KRH buffer and a sample of ddH_2O to serve as blank. The dilution series were used to set up a standard curve in order to calculate the glycerol concentrations of the samples (equation 3.1). The absorbance was measured at 540 nm in spectrophotometer Spectra Max Plus 384.

Equation 3.1: $$\frac{(Asample - Ablank)}{(Astandard - Ablank)} \; x \; Concentration \; of \; standard$$

3.15 Statistical analysis

All statistical analyses were performed in R studio. Shapiro-Wilk test was performed to check for normality and all variables from flow cytometry, gene expression, lipolysis and glucose uptake data were log transformed. Two-sided paired t-test was performed to compare macrophage populations and gene expression between SAT and VAT. Paired Wilcoxon Signed-rank test was performed to compare lipolysis and glucose uptake between SAT and VAT. It was performed Pearson and Spearman correlation analysis between flow cytometry, gene expression, lipolysis and glucose uptake data with clinical data.

4. Results

4.1 Comparison of monocytes, M1- and M2-like macrophages in SAT and VAT

Flow cytometry was used to assess whether there are fat depot specific differences with respect to macrophage infiltration. PBMC were isolated from human blood by density gradient centrifugation and the SVF obtained from SAT and VAT by collagenase digestion from a cohort of 21 severely obese patients undergoing bariatric surgery. Gating strategy to isolate total macrophage and monocyte population from one representative VAT sample is depicted in Figure 4.1.A, and gating strategy to quantify the fraction of monocytes, M1-like and M2-like macrophages from one representative PBMC, SAT and VAT sample is depicted in Figure 4.1.B.

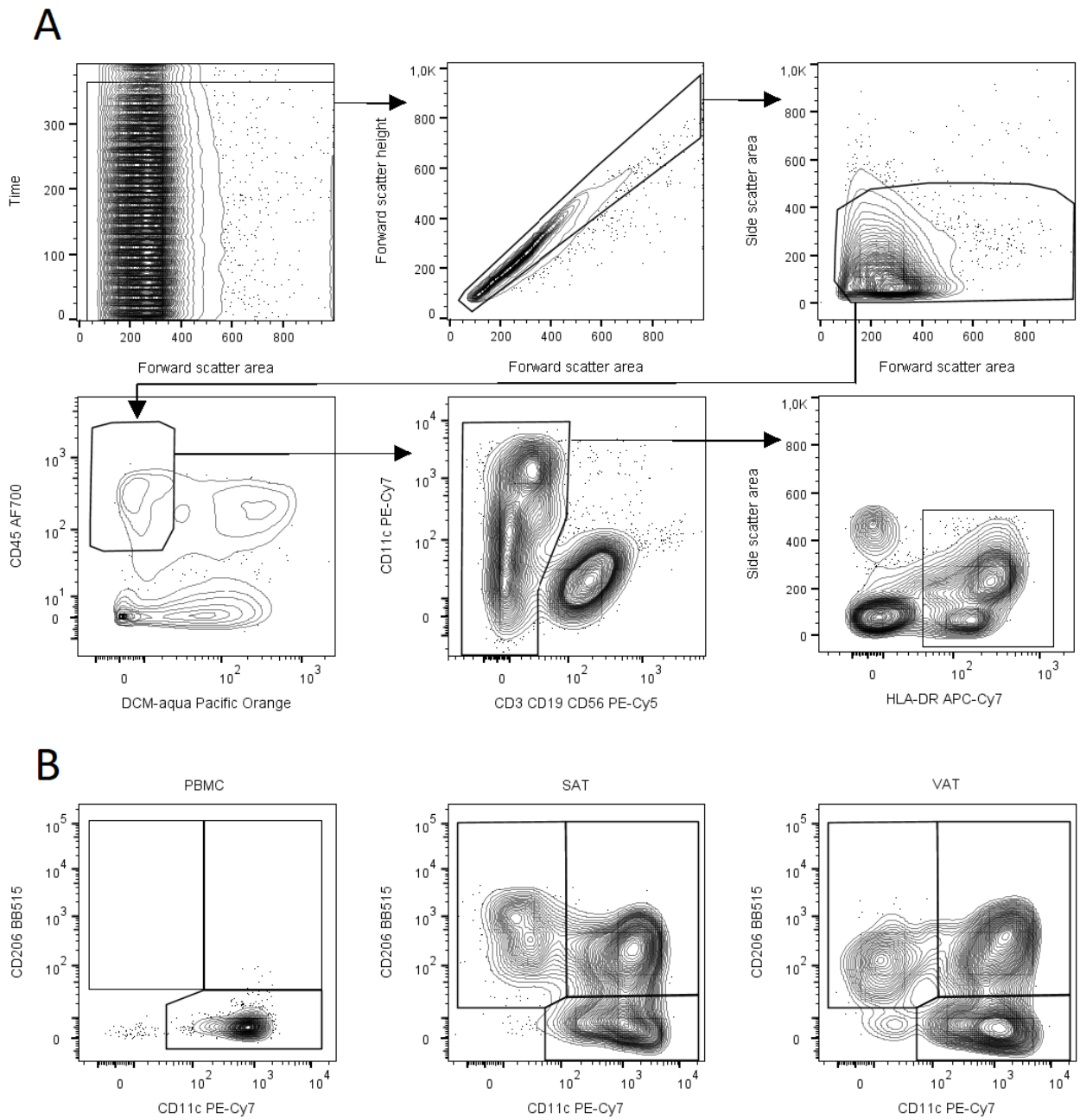

Figure 4.2. Gating scheme for isolating monocytes, M1- and M2-like macrophages. *A: First a time gate was applied to exclude electronic noise, then forward scatter area is plotted against forward scatter height to gate for single cells excluding any doublets, followed by plotting forward scatter area versus side scatter area to gate for lymphocytes and monocytes. Then cells positive for CD45 and negative for the dead cell marker DCM aqua was gated for followed by plotting CD3-CD19-CD56 PE-Cy5 against CD11c PE-Cy7 to exclude T- and B-lymphocytes and NK-cells respectively. Lastly HLA-DR APC-Cy7 was plotted against side scatter area to isolate the HLA-DR positive macrophages and monocytes. B: CD11c PE-Cy7 was plotted against CD206 BB515 to quantify the fraction of the CD11c+ CD206+ M1-like macrophages, CD11c- CD206+ M2-like macrophages and CD11c+ CD206- monocytes from the total macrophage and monocyte population.*

The macrophages and monocytes were isolated based on their expression of CD45 and HLA-DR, and absent of CD3, CD19 and CD56 expression. The different macrophage populations were then isolated and categorized based on the expression of CD11c and CD206; M1-like macrophages CD11c+CD206+, M2-like macrophages CD11c-CD206+ and monocytes CD11c+CD206-. First, we assessed the fraction of macrophages from the total of CD45+ cells in PBMC, SAT and VAT. We found that there was a significant ($p<0.001$) higher number (mean %, ± sd) of total macrophages in SAT (22.7 ± 8.0) and PBMC (23.5 ± 9.8) compared to VAT (10 ± 5.3) (Figure 4.2.A). The higher fraction in total macrophage and monocyte population seemed to arise from a significant higher fraction of monocytes in SAT versus VAT (Figure 4.2.B), indicating a higher infiltration of monocytes into SAT. However, the number of M2-like macrophages were higher in VAT than in SAT, but not enough to account for the difference in total macrophage and monocyte content. In PBMC, M2-like macrophages were only detected in a few samples and at a very low number. The fraction of M1-like macrophages was similar between SAT and VAT, and only present at a very low amount in peripheral blood (0.82 ± 0.7) which mostly contained the CD11c positive monocytes.

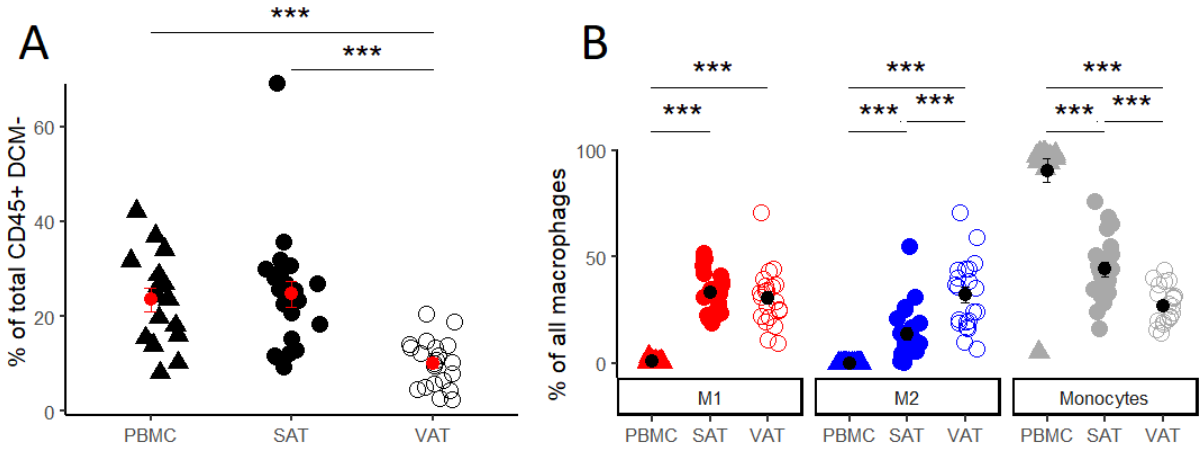

Figure 4.3. Macrophage populations from PBMC, SAT and VAT*. Scatter plot showing; A: The fraction of macrophages and monocytes in PBMC, SAT and VAT from the total of CD45+ viable cells isolated. B: The fraction of monocytes, M1-like and M2-like macrophages from the total macrophage and monocyte population in PBMC, SAT and VAT (n=21). *** = p<0.001.*

4.2 Characterizing the phenotype of monocytes, M1-like and M2-like macrophages

In order to assess whether the CD11c+CD206+ M1-like and CD11c-CD206+ M2-like macrophages exhibit a pro- and anti-inflammatory phenotype respectively, the expression of the established pro-inflammatory surface receptors such as CD14, CD16, CD40, CD44, CCR2, HLA-DR and the anti-inflammatory receptor CD163 was assessed by flow cytometric analysis. Most notable was the significant higher number of cells expressing the chemotactic receptor CCR2 (Lim, Yuzhalin et al. 2016) among the M1-like macrophages compared to the M2-like macrophages, in both SAT and VAT. Similarly, a high fraction of monocytes in SAT and VAT expressed CCR2 suggesting that these cells are recruited to the adipose tissue. There was also a significant higher number of the M1-like macrophages in VAT (90.9 ± 8.8) versus SAT (74,3 ± 27,5) expressing CCR2 suggesting that a higher fraction of the macrophages in VAT are recruited pro- inflammatory cells and not arise from proliferating resident cells. CD44, a receptor that is known to be involved in cell migration but also proliferation and activation of cells (Senbanjo and Chellaiah 2017), were found to be higher expressed on M1-like macrophages and monocytes in both SAT and VAT compared to M2-like macrophages, supporting that these cells are infiltrating pro-inflammatory cells. CD14, a pattern recognition receptor known to be involved in innate immune responses as a co-receptor for TLR`s (Kelley, Lukk et al. 2013) was higher expressed on both M1-like and M2-like macrophages compared to monocytes in VAT, and significantly higher on the M2-like macrophages in VAT versus M2-like macrophages in SAT, supporting a more inflammatory phenotype in VAT. However, no significant differences were found between M1-like and M2-like macrophages. CD163, which is best known for its homeostatic and anti-inflammatory functions (Etzerodt and Moestrup 2013), was significantly higher expressed on M2-like versus M1-like macrophages in VAT supporting an anti-inflammatory phenotype of M2-like macrophages. However, this was not observed in SAT. Additionally, monocytes expressed significantly lower levels of CD163 in all tissues. There is no significant difference in the expression levels of the pro-inflammatory receptors CD16, CD40 and HLA-DR between monocytes, M1-like and M2-like macrophages and between the different tissues. However, a large variation in the expression levels was observed, indicating different subpopulations with pro- and anti-inflammatory characteristic within the populations of M1- and M2- like macrophages. The intensity plot in Figure 4.3.H from one representative VAT sample are

illustrating the vast differences in expression of CCR2 on monocytes and M1-like macrophages compared to M2-like macrophages.

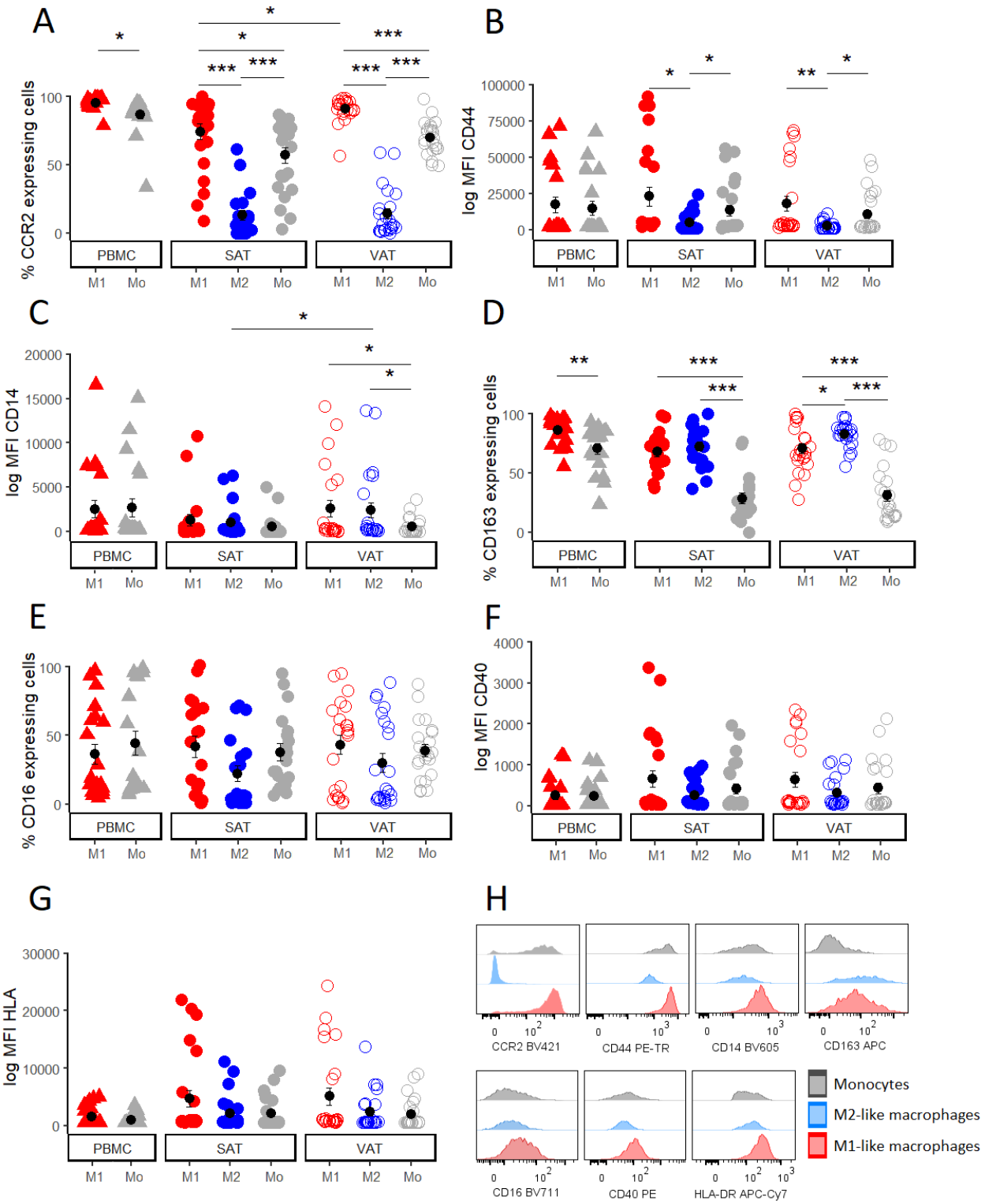

Figure 4.4. Expression of surface receptors on Monocytes (Mo), M1-like and M2 like macrophages. *A, D and C: Scatter plot showing the percentage of cells expressing the proteins CCR2(A), CD44(B), CD14(C) and CD163(D) on Monocytes (grey), M1-like (red) and M2-like (blue) macrophages. B, C, F and G: Scatter plot showing the log mean fluorescence intensity (MFI)*

*from staining of CD44 (B), CD14 (C) and CD40(F), and HLA-DR (G) on Monocytes, M1-like and M2-like macrophages in PBMC, SAT and VAT. H: Intensity plot from the staining of proteins in A-G from a representative VAT sample. Black dot represents mean and error bar represent SEM (n=21). * = p<0.05, ** = p<0.01, *** = p<0.001.*

4.3 Quantifying M1- and M2-like macrophages in normal weight, obese and T2DM subjects

Next, we wanted to investigate whether there was a different in composition of M1- and M2-like macrophages in SAT and VAT of normal weight subjects, obese or obese subjects diagnosed with T2DM. We included 3 normal weight subjects undergoing cholecystectomy to represent the control group and identified 9 subjects diagnosed with T2DM from our cohort of severely obese bariatric surgery patients. Data from 4 of the subjects in the obese group were excluded from the analysis due to a low number of cells. We observed no significant differences in the fraction of each cell type within SAT or VAT between normal weight, obese or subjects with T2DM (Figure 4.4).

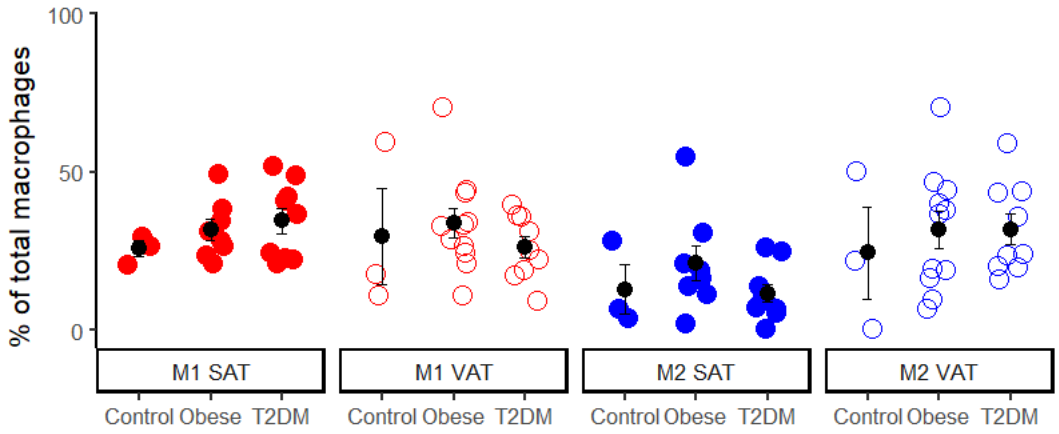

Figure 4.5. Macrophage populations in SAT and VAT of normal weight (control), obese and T2DM subjects. *Scatter plot showing the percentage of M1- and M2-like macrophages of the total macrophage population In SAT and VAT in normal weight (control, n=3), obese(n=8) and T2DM(n=9) subjects. Black dot represents mean and error bar represent SEM. ** = p<0.01.*

4.4 Depot specific associations of ATM populations with clinical parameters.

We also wanted to investigate whether the composition of pro-inflammatory M1-like and anti-inflammatory M2-like macrophages from adipose tissue was associated with clinical parameters relevant for systemic insulin resistance or the lipid profile, and markers of inflammation measured in peripheral blood. For 4 of the subjects, we were not able to provide clinical data. The analysis includes 16 subjects in total from the control group, obese and obese with T2DM. All variables were log transformed due to non-normally distributed data and there was performed a Pearson correlation analysis (Figure 4.5). Interestingly, the pro-inflammatory M1/M2-ratio in VAT was significantly correlated with the circulating markers of inflammation, CRP (R^2 = 0.535, p = 0.032) and leukocytes (R^2 = 0.763, p = 0.0006). Similarly, there was a significant, negative correlation of M2-like macrophages in VAT with CRP and leukocytes, indicating that macrophage polarization towards a more pro-inflammatory phenotype is associated with systemic inflammation. Moreover, there was a positive, but non-significant correlation of leukocytes and monocytes in VAT, suggesting a higher infiltration of monocytes into VAT than in SAT in the setting of inflammation. Insulin correlated positive with the anti-inflammatory M2-like macrophages (R^2 = 0.533, p = 0.033) in SAT and negatively with the pro-inflammatory M1/M2-ratio (R^2 = -0.569, p = 0.021). The same association was seen for HOMA-IR, although not significant (R^2 = 0.437, p = 0.090 and R^2 = -0.474, p = 0.063). Interestingly, this association was not seen in VAT. There were no significant correlations between the macrophage populations and the lipid profile in the blood or BMI and age. Because some of the variables were not normally distributed, we also performed a Spearman correlation, which showed the same trends, although none remained significant.

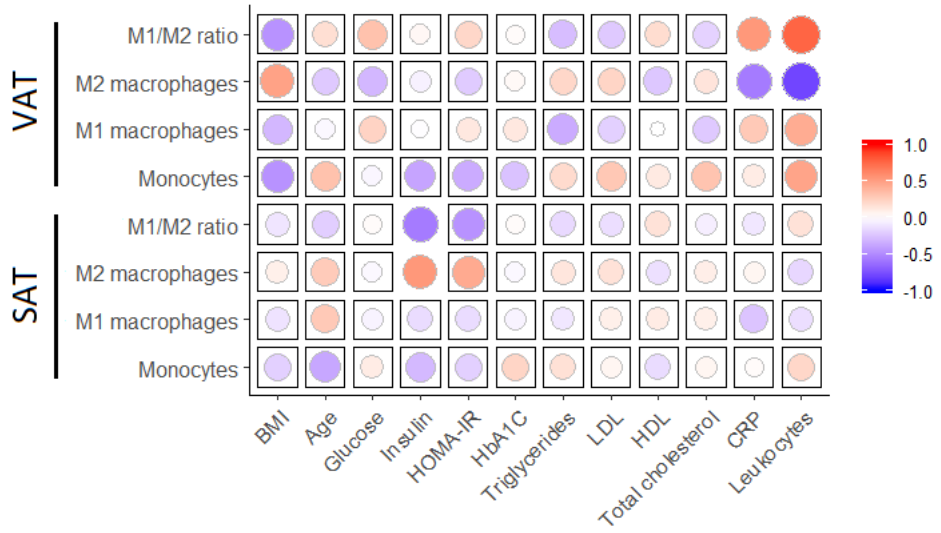

Figure 4.6. Correlation plot of macrophage populations versus clinical parameters. *Pearson correlation of Monocytes, M1-, M2-like macrophages and M1/M2 ratio with clinical parameters measured in peripheral blood (n=16). Size and color of circles indicate correlation coefficients and squares indicate non-significant correlations (p>0.05)*

4.5 Depot specific differences in expression levels of pro- and anti-inflammatory genes

In addition to analyzing the inflammatory phenotype of macrophages in adipose tissue, we wanted to assess how the expression level of genes relevant for adipose tissue inflammation differed between SAT and VAT in a cohort of 54 severely obese subjects. The expression levels were quantified at the mRNA level by RT-qPCR. The fold change ($2^{-\Delta\Delta Ct}$) was calculated relative to IPO8 as reference gene and normalized to the mean of the SAT samples, and then log transformed due to non-normally distributed data. There was no significant difference in the expression levels of the pro-inflammatory genes TNF (Figure 4.6.A), IFN-gamma (C) and IL6 (D) between SAT and VAT. However, the chemotactic ligand MCP-1 (B) (Kanda, Tateya et al. 2006) and the macrophage associated protein CD68 (H) was significantly higher expressed in SAT, which supports the findings from the flow cytometry analysis (Figure 4.2.A) that total macrophage content is higher in SAT than VAT. The lipid receptor TREM2 (Jaitin, Adlung et al. 2019) is considered to have an anti-inflammatory role in maintaining metabolic homeostasis. We observed that TREM2 was significantly higher expressed in SAT, suggesting a less inflammatory profile in SAT versus VAT. Contrary, CD163 (I), which is also considered to be involved in anti-inflammatory responses (Etzerodt and Moestrup 2013), was significantly higher expressed in VAT than in SAT, contradicting the suggested difference in

the inflammatory profile between SAT and VAT. There were no significant differences in the expression levels of TREM1 (E), or NR4A1 (G) between SAT and VAT.

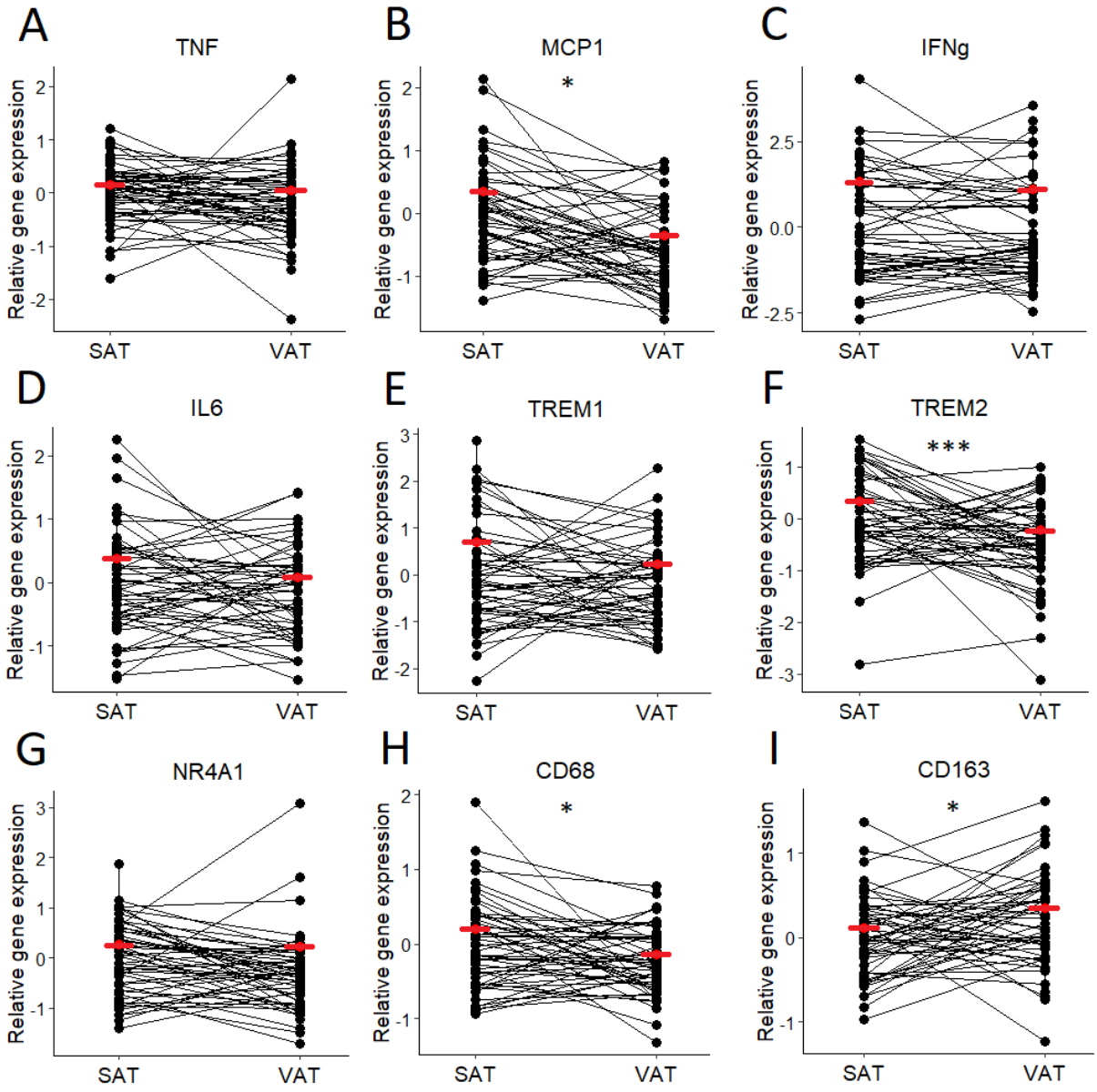

Figure 4.7. Relative expression level of pro- and anti-inflammatory genes between SAT and VAT. *The expression levels of the pro- inflammatory genes TNF (A), MCP1 (B), IFN-gamma (C), IL6 (D), the anti-inflammatory genes TREM1 (E), TREM2 (F), The adipocyte specific transcription factor Nr4A1 (G) and the macrophage specific proteins CD68 (H) and CD163 (I) were analyzed by qPCR and results are presented as log transformed fold change ($2^{-\Delta\Delta Ct}$) of the target gene relative to the reference gene IPO8. The expression levels were normalized to the mean of the SAT samples. Red line indicates the mean and the line is connecting the SAT and VAT sample from the same patient (n=54). * = p<0.05, ** = p<0.01, *** = p<0.001.*

4.6 Co-expression of pro- and anti-inflammatory genes within and between fat depots

Next, we wanted to assess the inflammatory profile in SAT and VAT by analyzing patterns of co-expression among the pro- and anti-inflammatory genes. A strong significant correlation between the macrophage associated protein CD68 with CD163, TREM1, TREM2 and MCP1 in SAT could indicate that the immune cells infiltrating SAT present with an anti-inflammatory gene expression pattern. (Figure 4.7.A) CD68 also correlate strongly with CD163 and TREM2 in VAT but not with MCP1 or TREM1. In addition, NR4A1, which expression is found to be associated with impaired adipose tissue plasticity and inflammation (Zhang, Federation et al. 2018), was significantly correlated with the pro-inflammatory genes TNF, IFN-γ and IL6 supporting an inflammatory response in VAT (Figure 4.7.B) related to impaired adipose tissue plasticity. We also wanted to assess whether upregulation of pro- or anti-inflammatory genes in one fat depot is reflected by upregulation of the same gene in the other depot, or is reflected by up- or down regulation by one of the other genes (Figure 4.8). In fact, the expression of NR4A1 and the pro-inflammatory genes TNF, MCP1, IFN-γ, and IL6 were found to exhibit a significantly correlated expression between SAT and VAT. Most prominent was the strong correlation of IFN-γ, which is known as the most important cytokine for activation of pro-inflammatory M1-like macrophages (O'Rourke, White et al. 2012). This suggests that inflammation in one fat depot was reflected by inflammation in the other depot as well. Interestingly, the upregulation of NR4A1 in one depot was reflected by upregulation of IFN-γ in the other depot, supporting the notion that NR4A1 plays a role in adipose tissue inflammation.

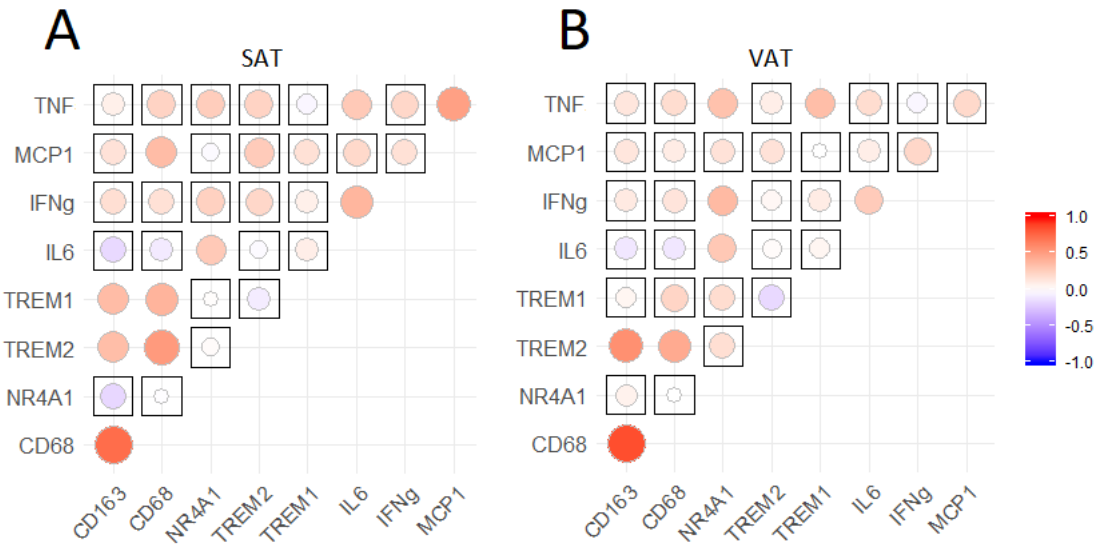

Figure 4.8. Co-expression of pro- and anti-inflammatory genes in SAT and VAT. *Correlation plot showing the Person correlation between expression levels of the Pro-inflammatory genes TNF, MCP1, IFN-gamma, IL6, the anti-inflammatory genes TREM1, TREM2, the transcription factor Nr4A1 and the genes for the macrophage associated receptors CD68 and CD163 in SAT (A) and VAT (B) (n=54). Size and color of circles indicate correlation coefficients and squares indicate insignificant associations (p>0.05).*

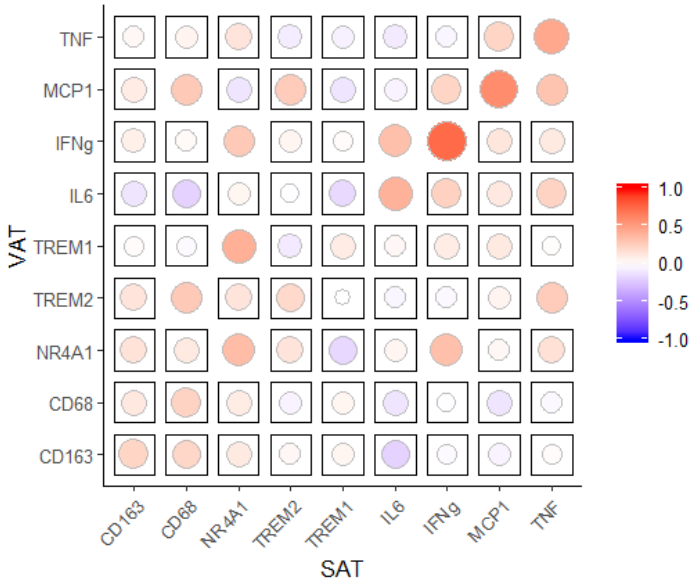

Figure 4.8. Correlation between pro- and anti-inflammatory genes expressed in SAT and VAT. *Correlation plot indicating the Pearson correlation of the Pro- inflammatory genes TNF, MCP1, IFN-gamma, IL6, the anti-inflammatory genes TREM1, TREM2, the transcription factor Nr4A1 and the genes for the macrophage associated receptors CD68 and CD163 expressed in SAT and VAT (n=54). Size and color of circles indicate correlation coefficients and squares indicate insignificant associations (p>0.05).*

4.7 Associations between the expression levels of pro- and anti-inflammatory genes with clinical data.

In order to establish whether a pro-inflammatory gene expression pattern in adipose tissue is associated with systemic insulin resistance, an unhealthy lipid profile or markers of inflammation measured in peripheral blood, a correlation analysis was performed. Interestingly, HOMA-IR and HbA1C, a measure of insulin resistance and glucose intolerance, respectively, and triglyceride levels were all found to be positively correlated with CD68 and CD163 expression in SAT, indicating a higher number of macrophages in SAT of insulin resistant subjects. TREM2 expression in SAT also correlated with HOMA-IR (R^2 = 0.408, p = 0.002) and HbA1C (R^2 = 0.312, p = 0.024) suggesting a more anti-inflammatory profile in SAT of insulin resistant subjects. Interestingly, IL6 correlated negatively with HOMA-IR in SAT (R^2 = -0.305, p = 0.028), and a similar trend was observed in VAT (R^2 = -0.244, p = 0.081), although not significant. Moreover, IL6 expression in SAT (R^2 = 0.284, p = 0.041) and VAT (R^2 = 0.255, p = 0.067) associated positively with HDL, an indicator of a healthy lipid profile, which supports the notion of a pleiotropic function of this cytokine beyond its role in inflammation (Kurauti, Costa-Junior et al. 2017). It is noteworthy that there are no associations of HOMA-IR, HbA1C or triglycerides with CD68 and CD163 or the anti-inflammatory gene TREM2 in VAT. A significant correlation of MCP1 (R^2 = 0.412, p = 0.002) with BMI suggests a higher infiltration of monocytes into VAT in the setting of obesity. In SAT, however, BMI only showed a significant association with CD68. It is also intriguing that expression of NR4A1 (R^2 = 0.294, p = 0.034) and also CD163 in VAT correlated positively with CRP. In addition, there, was a positive but not significant association of the pro-inflammatory genes TNF, MCP1 and IFN-gamma in VAT with CRP, suggesting a link between systemic inflammation and AT inflammation in VAT.

To summarize, this analysis suggests that insulin resistance and an unhealthy lipid profile is characterized by a pattern of anti-inflammatory gene expression in SAT and an absent of this pattern in VAT, supporting the conclusion from the flow cytometry data that insulin resistance is associated with a higher proportion of M2-like macrophages in SAT, which is not seen in VAT. The results from the gene expression analysis also suggest that a pro-inflammatory gene expression pattern in VAT is associated with systemic inflammation,

which supports the conclusion from the flow cytometry data that the pro-inflammatory M1/M2-ratio are associated with systemic inflammation.

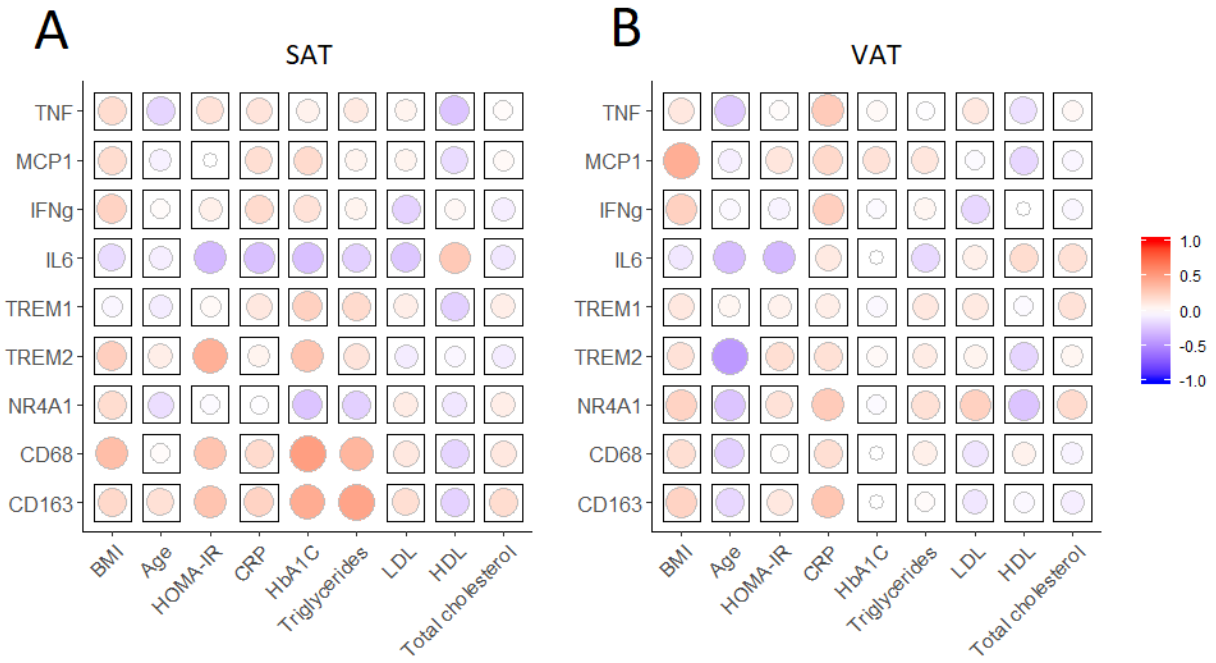

Figure 4.9. Correlation plot of pro- and anti-inflammatory gene expression in SAT and VAT with metabolic parameters. *Correlation plot indicating the Pearson correlation of the Pro- inflammatory genes TNF, MCP1, IFN-gamma, IL6, the anti-inflammatory genes TREM1, TREM2, the transcription factor Nr4A1 and the macrophage associated receptors CD68 and CD163 expressed in SAT and VAT with metabolic parameters (n=54). Size and color of circles indicate correlation coefficients and squares indicate insignificant associations (p>0.05).*

4.8 Comparison of the rate different adipose tissue depots mobilize fatty acids.

Further we wanted to assess functional characteristics of isolated mature adipocytes. From a cohort of 21 severely obese patients undergoing bariatric surgery, the rate of glycerol release were measured in freshly isolated adipocytes from SAT and VAT, with the aim of comparing the rate in which adipocytes mobilize their fatty acids through lipolysis between the two depots. A correlation analysis (Figure 4.11) was also performed to assess whether the degree of lipolysis associated with systemic insulin resistance, metabolic dysregulation or measures of systemic inflammation. A pairwise comparison revealed that the basal rate of lipolysis was similar between the two tissues and there was a significant increase in response to isoprenaline stimulation in both tissues (Figure 4.11). As expected, the rate of

which isoprenaline stimulation increased lipolysis was significantly higher in VAT (Wilcox test p<0.001) indicating that fatty acids from VAT is first mobilized in periods of energy demand (Bodis and Roden 2018).

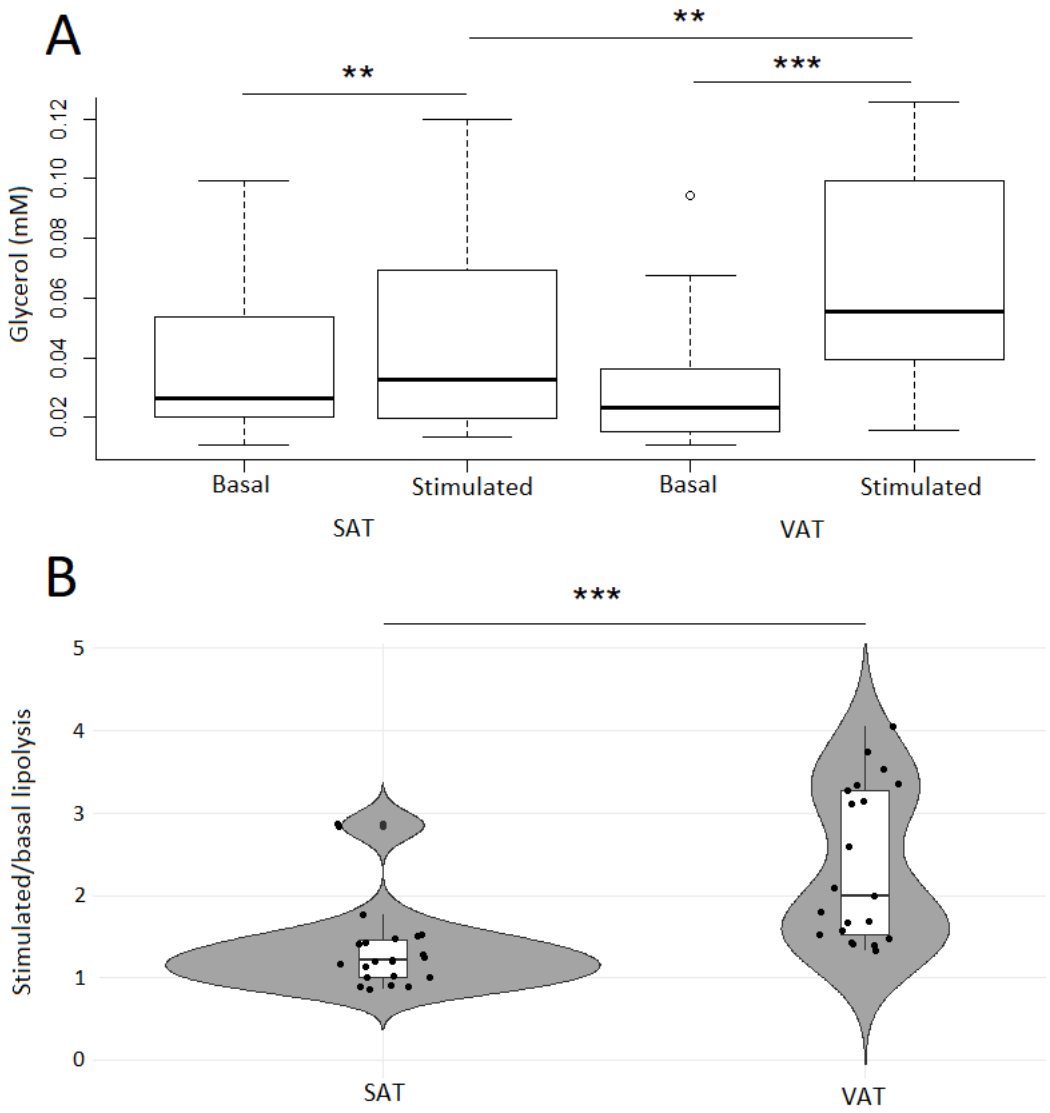

Figure 4.10. The rate of basal and stimulated lipolysis in SAT and VAT. *A: Boxplot showing the rate of lipolysis in SAT and VAT in basal and in isoprenaline stimulated conditions measured by glycerol release. B: Violin plot showing the increase in rate of lipolysis in response to isoprenaline stimulation in SAT and VAT (n=21). ** = p<0.01, *** = p<0.001.*

The correlation analysis revealed a negative correlation of LDL (R^2 = -0.545, p = 0.011) and total cholesterol levels (R^2 = -0.497, p = 0.028) in blood with the lipolytic response in VAT.

This was not observed in SAT, instead the lipolytic response in SAT was correlated with triglycerides (R^2 = 0.536, p = 0.012), suggesting a negative contribution of the lipolytic response in SAT with respect to metabolic syndrome. Insulin levels and HOMA-IR also associated negatively with both basal (R^2 = -0.536, p = 0.012 & R^2 = -0.479, p = 0.027) and stimulated lipolysis (R^2 = -0.619, p = 0.002 & R^2 = -0.579, p = 0.005) in VAT, but not to the lipolytic response. This contradicts the notion that elevated basal levels of lipolysis in VAT is exacerbating insulin resistance and T2DM by promoting ectopic lipid accumulation (Bodis and Roden 2018).

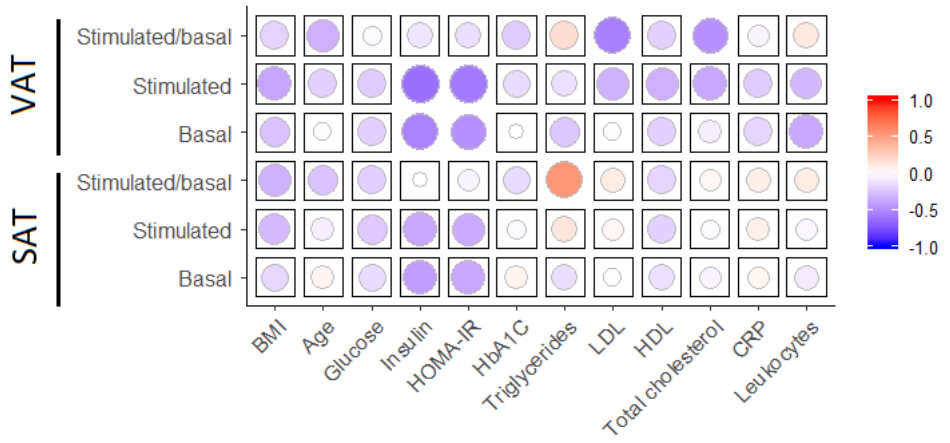

Figure 4.11. Correlation plot of lipolysis versus clinical parameters. *Correlation plot indicating Person correlation between the rate of lipolysis and metabolic parameters measured in blood in addition to BMI and Age (n=21). Size and color indicate correlation coefficients and squares indicate insignificant associations (p>0.5).*

4.9 Glucose uptake and insulin sensitivity between different adipose tissue depots.

Next, we assessed the glucose uptake and insulin sensitivity by measuring uptake of C-14 glucose in freshly isolated adipocytes from the same cohort as the lipolysis assay including one additional sample. Uptake of the radioactive glucose was measured by scintillation counting and the results presented as disintegrations per minute in Figure 4.12.A. Both adipose tissue depots responded significantly to insulin stimulation, and as expected both the basal and stimulated glucose uptake was elevated in VAT compared with SAT in our cohort (Westergren, Danielsson et al. 2005). The response to insulin stimulation on glucose uptake was, however, similar between the two depots (Figure 4.12.B).

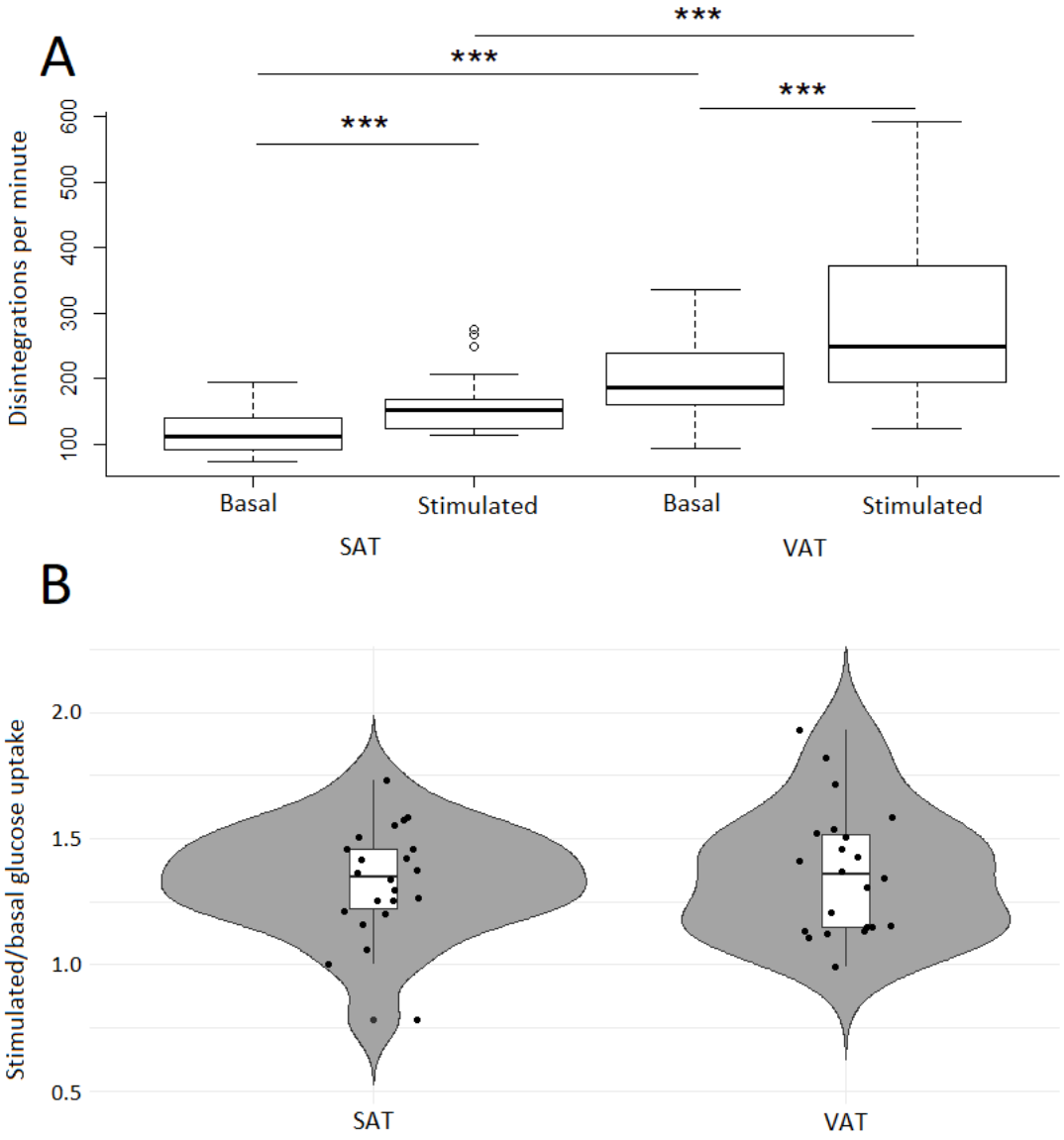

Figure 4.12. Glucose uptake in isolated adipocytes from SAT and VAT. *Uptake of C-14 glucose in freshly isolated adipocytes from SAT and VAT of severely obese subjects were measured by scintillation counting and results presented as disintegrations per minute. A: Boxplot showing the degree of glucose uptake in SAT and VAT under basal and insulin stimulated conditions. B: Violin plot comparing the fold increase in glucose uptake in response to insulin stimulation in SAT and VAT (n=22). *** = p<0.001.*

We also performed a correlation analysis of glucose uptake and insulin sensitivity in adipose tissue versus metabolic parameters measured in blood in order to reveal whether insulin resistance and glucose intolerance in adipose tissue is associated with systemic measures of insulin resistance or other indicators of metabolic syndrome (Figure 4.13). We found a significant correlation of basal glucose uptake in VAT with HDL (R^2 = 0.459, p = 0.036) suggesting a beneficial effect on the lipid profile in blood. Moreover, a negative, but not significant, correlation of glucose uptake with glucose levels in blood was found, supporting that glucose intolerance in adipose tissue is reflective of glucose intolerance at the systemic level.

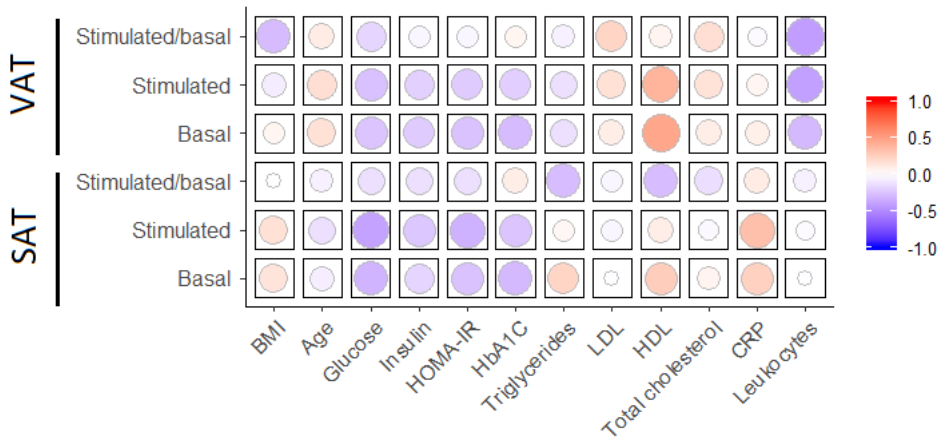

Figure 4.13. Correlation plot of glucose uptake versus clinical parameters. *Correlation plot indicating Person correlation of glucose uptake and insulin sensitivity versus metabolic parameters measured in blood in addition to BMI and Age (n=22). Size and color indicate correlation coefficients and squares indicate insignificant associations (p>0.5).*

Both lipolysis and glucose uptake are essential processes in regulating the whole-body energy homeostasis. Therefore, we wanted to investigate how the two different processes associated by doing a correlation analysis (Figure 4.14). The results showed that the response of glucose uptake on insulin stimulation associated negatively with lipolytic response in VAT (R^2 = -0.459, p = 0.036). Contrary, the basal level of lipolysis showed a positive association with insulin sensitivity (R^2 = 0.440, p = 0.046) in VAT, that contradicts previous reports showing that insulin resistance in VAT is associated with elevated levels of basal lipolysis (Bodis and Roden 2018).

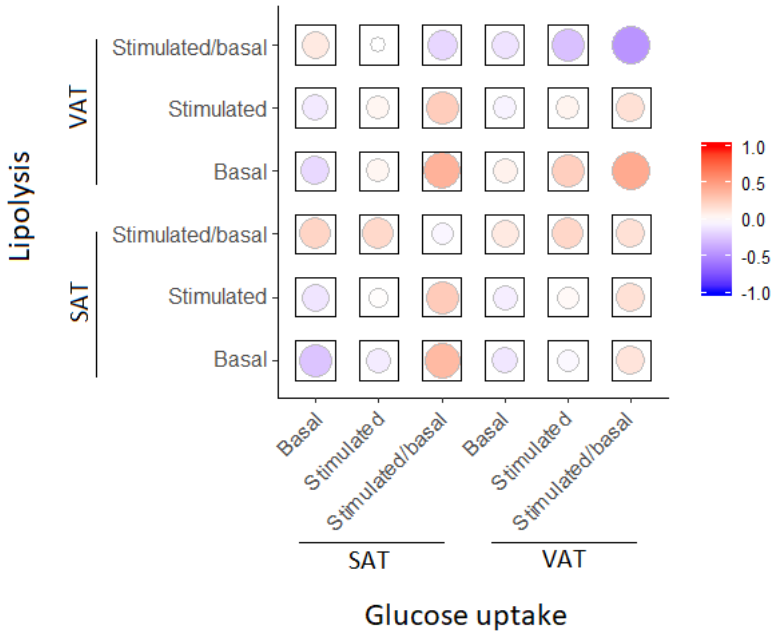

Figure 4.14. Correlation plot of glucose uptake versus lipolysis. *Person correlation of glucose uptake versus the rate of lipolysis in SAT and VAT (n=21). Size and color indicate correlation coefficients and squares indicate insignificant associations (p>0.5).*

5. Discussion

Adipose tissue inflammation has been pointed out as a plausible mechanistic link connecting obesity and associated diseases such as insulin resistance and T2DM. It is now widely accepted that macrophages and other immune cells infiltrate adipose tissue at a high rate and are contributing to a chronic state of inflammation in the tissue. However, the relative contribution of different immune cell populations is still heavily debated, and there is a lack of consensus with respect to which molecular players are contributing to the worsened metabolic phenotype. The aim of this thesis was to investigate fat depot-specific differences with respect to adipose tissue inflammation, and to phenotypically characterize the ATM populations. We also wanted to study whether skewing towards a more pro-inflammatory macrophage population is associated with systemic insulin resistance, inflammation, or an unhealthy lipid profile. Furthermore, we performed functional analyses in freshly isolated mature adipocytes to investigate how glucose uptake and lipolysis are associated with systemic insulin resistance, inflammation and lipid profile.

5.1 SAT contains a higher fraction of ATM than VAT

Insulin resistance has been associated with infiltration of macrophages in both SAT and VAT, observed both in HFD fed mice and obese humans (Bodis and Roden 2018). In particular, infiltration into VAT has been associated with a worsened metabolic phenotype (Lebovitz and Banerji 2005), although the relative contribution of each fat depot has been heavily debated. In our study we found that SAT contains a significant higher fraction of total macrophages and monocytes than VAT. This was also found in another study that involved 29 obese bariatric surgery patients where macrophages and monocytes were also characterized by the expression of CD11c and CD206 (Wentworth, Naselli et al. 2010). We also assessed the gene expression in SAT and VAT and found that CD68 and MCP1, but also TREM2 is higher expressed in SAT than VAT, which supports that macrophages are more abundant in SAT. Conversely, a study done in 55 morbidly obese gastric surgery patients, where the surface protein HAM56 was used to characterize macrophages by immunohistochemistry, found the number of infiltrating macrophages to be twice as high in

VAT as in SAT (Cancello, Tordjman et al. 2006), whereas a study performed in 10 lean cholecystectomy patients failed to find any differences between SAT and VAT (Koenen, Stienstra et al. 2011). Moreover, our gene expression data showed that CD163 are more highly expressed in VAT than in SAT, which may rise doubt about whether the macrophages are likely to be more abundant in SAT. The discrepancy between different studies reporting ATM compositions highlights the need for a more unifying concept on how to best identify ATMs.

5.2 Alternatively activated M2-like macrophages are more abundant in VAT than SAT

It is well known that there are different subsets of macrophages in adipose tissue with different functional properties, and earlier studies have characterized a subset of CD11c+CD206+ ATM that shows features of classically activated macrophages (M1) and a subset of CD11c-CD206+ ATM that shows features of alternatively activated macrophages (M2) (Wentworth, Naselli et al. 2010). We looked at how these populations of macrophages were distributed in the two fat depots and found the alternatively activated M2-like macrophages to be significantly more abundant in VAT. These findings were supported by the gene expression analysis showing a higher expression of the anti-inflammatory marker CD163 in VAT. Contrary, the monocytes were more abundant in SAT compared to VAT. However, there was no difference in the number of M1-like macrophages between SAT and VAT.

If inflammation in VAT is more closely associated with insulin resistance than in SAT, we could expect a higher number of the pro-inflammatory M1 macrophages in VAT of subjects with T2DM. We therefore analyzed the composition of M1 and M2 macrophages after separating the subjects diagnosed with T2DM from our cohort of severely obese subjects. In addition, we included three subjects undergoing cholecystectomy with a BMI in the range 22-29 kg/m^2 to represent the control group. Somewhat unexpected, we could not find any significant differences in number of M1- or M2-like macrophages between the control group, the T2DM patients and the obese group without T2DM. A small sample size could explain the lack of differences observed.

5.3 High expression of CCR2 by M1-like macrophages supports their pro-inflammatory identity.

There is still a debate on how to best characterize pro- and anti-inflammatory macrophages in adipose tissue, and studies have shown that the alleged CD11c+CD206+ M1-like macrophages also exhibit characteristics of anti-inflammatory M2-like macrophages such as high mitochondrial copy number and high expression of the anti-inflammatory cytokine IL-10 (Vats, Mukundan et al. 2006), (Mantovani, Sica et al. 2004), (Kim, Zhang et al. 2004). Therefore, we sought to confirm the pro- and anti-inflammatory phenotype of M1-like and M2-like macrophages from SAT and VAT by the expression of additional surface receptors. Most strikingly, the pro-inflammatory marker CCR2 was found to be highly expressed by M1-like macrophages and to some extent on the monocytes but was almost absent on the M2-like macrophages. Interestingly, the level of ATM CCR2 expression varied between the fat depots, with CCR2 consistently expressed by a higher fraction of the M1-like macrophages in VAT, while there was a great variation in the number of CCR2 expressing M1-like macrophages in SAT, which supports a more pro-inflammatory profile in VAT. A similar pattern was observed for the monocytes. CD44 was also found to be higher expressed by both M1-like macrophages and monocytes in both SAT and VAT. CD44 is also a receptor involved in cell migration and an important mediator in the cell responding to pro-inflammatory stimuli (Lim, Yuzhalin et al. 2016), (Senbanjo and Chellaiah 2017). Studies have found the ratio of anti-inflammatory M2-like macrophages versus M1-like macrophages to be significantly higher in adipose tissue of CD44 knock-out mice fed a HFD, which supports that CD44 is facilitating infiltration of M1-like macrophages into adipose tissue (Kang, Liao et al. 2013). Interestingly, the M1-like macrophages displayed a great variation in expression levels of CD44 between the subjects. The alleged anti-inflammatory marker CD163 was highly expressed in both M1-like and M2-like macrophages in SAT and VAT, and showed only a marginal higher expression in M2-, relative to M1-like macrophages in VAT. This suggests that CD163 is probably not an appropriate marker to distinguish between pro- and anti-inflammatory macrophages in adipose tissue. In conclusion, the high expression of CCR2 supports a pro-inflammatory identity of M1-like macrophages. Moreover, in animal models of obesity, it has been found that silencing CCR2 reduces macrophage number and inflammation in adipose tissue and also improve insulin sensitivity (Kim, Chung et al. 2016).

However, the high variability in expression of CD14, CD16, CD40, CD44 and HLA-DR on both M1- and M2-like macrophages suggests a broad spectrum of activation states or the existence of different subgroups of cells within these cell populations.

5.3 Elevated levels of insulin and HOMA-IR are associated with M2-like macrophages in SAT

Similar studies have shown that insulin resistance is associated with increased numbers of CD11c+CD206+ M1- like macrophages and also with the pro-inflammatory M1/M2 ratio in both SAT and VAT (Wentworth, Naselli et al. 2010). We performed a person correlation analysis to investigate whether the different macrophage populations or the M1/M2 ratio are associated with systemic insulin resistance or other clinical parameters relevant for metabolic syndrome in our cohort. Surprisingly, the M1/M2 ratio in SAT correlated negatively with HOMA-IR. Although this association was not significant, there was clearly a trend, which was supported by a strong significant negative association of insulin levels with the M1/M2 ratio and the positive association of CD11c-CD206+ M2-like macrophages with insulin. Similar associations between insulin resistance and macrophage populations were not found in VAT. The gene expression analysis supports that insulin resistance is associated with increased number of M2-like macrophages in SAT by the positive association of CD68, CD163 and TREM2 with HOMA-IR and HbA1C, which were not detected in VAT. Although CD68 and CD163 are not specific for M2-like macrophages, TREM2 has been recognized for its role in anti-inflammatory M2-like macrophages by its ability to suppress inflammatory responses by blocking toll-like receptor signaling (Turnbull, Gilfillan et al. 2006), (Zhong, Chen et al. 2015) and subsequent secretion of the proinflammatory cytokines IL-1b, IL6 and iNOS. Moreover, studies in mice have found TREM2 to be a positive regulator of adipogenesis, and TREM2 KO-mice have been shown to have increased obesity, insulin resistance and impaired adipose tissue remodeling (Liu, Li et al. 2019). This suggests that TREM2-expressing M2-like macrophages could be involved in a protective mechanism to cope with insulin resistance by regulating adipogenesis and inflammation (Liu, Li et al. 2019), and our results indicate that this mechanism may be less active in VAT.

We also found that M1/M2 ratio in VAT strongly associated with CRP and leukocytes while M2 macrophages associated negatively with the same parameters, which supports the hypothesis that adipose tissue inflammation can promote systemic inflammation (Fontana, Eagon et al. 2007). This was further supported by the gene expression analysis showing that NR4A1, TNF, MCP1 and IFN-γ expression in VAT associated with systemic CRP levels. Contrary, from experiments in rats it has been reported that CRP are able inhibit the differentiation of monocytes into M2-like macrophages and instead promote polarization of monocytes and M2-like macrophages into a M1-like phenotype suggesting that systemic inflammation can promote adipose tissue inflammation (Devaraj and Jialal 2011). However, the fact that there was no correlation between M1/M2 ratio in SAT with neither CRP nor leukocytes raise doubt about the direction of causality.

5.3 Pro-inflammatory gene expression is reflected in both fat depots

The expression levels of the pro-inflammatory genes, TNF, MCP1, IFN-γ, IL6, and also the transcription factor NR4A1, were strongly associated between SAT and VAT suggesting that inflammation in one fat depot is reflected by inflammation in the other depot as well. Although the pro-inflammatory gene expression pattern was mostly similar between the two depots, TREM1 deviated from this pattern by its strong association with the anti-inflammatory receptor CD163 in SAT. In VAT, there was a stronger association of the transcription factor NR4A1 with the pro-inflammatory genes TNF, IFN-γ and IL6 than in SAT. It has been suggested that adipose tissue inflammation and insulin resistance arise when the adipocyte hyperplastic response is insufficient to accommodate the metabolic stress of caloric excess as observed in both obesity and lipodystrophy (Wang, Tao et al. 2013), (Pasarica, Xie et al. 2009). NR4A1 has been described as a negative regulator of adipocyte hyperplasia suggesting a link to adipose tissue inflammation and T2DM (Zhang, Federation et al. 2018). The association with pro-inflammatory genes in our study supports a role for NR4A1 in adipose tissue inflammation, although we could not find an association with insulin resistance (measured by HOMA-IR). Interestingly, the expression of IL6 negatively correlated with HOMA-IR in both SAT and VAT, contradicting the traditional viewpoint of IL6 as an important pro-inflammatory mediator in promoting insulin resistance (Bastard, Maachi et al.

2002). While it was earlier believed that secreted IL6 had mostly negative effect on glucose homeostasis by affecting insulin signaling and promoting insulin resistance, particularly in the liver (Klover, Zimmers et al. 2003). Recent studies have discovered an important role of IL6 in regulating expression of insulin degrading enzyme and facilitating insulin clearance to prevent sustained exposure to high levels of insulin and consequently desensitization of the signaling pathway (Kurauti, Costa-Junior et al. 2017). This has been supported by studies showing that impairment in insulin-degrading enzyme are associated with insulin resistance (Karamohamed, Demissie et al. 2003). Moreover, it has been shown that IL6 primes macrophages to IL4 mediated polarization towards the M2-like phenotype by inducing the expression of IL4R-α through STAT3-mediated activation of IL4rα promoter (Mauer, Chaurasia et al. 2014). Interestingly, it has also been found that some of the beneficial effect exercise has on metabolic health is mediated through IL6 released into circulation from contracting muscle, influencing metabolism in distant tissue and organs (Pedersen and Fischer 2007). This indicates that the role of IL6 is likely to be both context and tissue dependent (Mauer, Denson et al. 2015) and more research should be put into figuring out the characteristic of the different actions of IL6.

5.4 VAT has a higher glucose uptake and are more sensitive to lipolytic stimulation.

In this study we have demonstrated that both basal and insulin stimulated glucose uptake is higher in VAT than SAT in our cohort of obese subjects. This has also been found in other studies (Christen, Sheikine et al. 2010), (Westergren, Danielsson et al. 2005). The increased stimulated levels of glucose uptake are likely caused by elevated levels of GLUT4 expression in VAT relative to SAT (Westergren, Danielsson et al. 2005). Elevated basal levels of glucose uptake could be caused by increased expression of GLUT1, although that has not been confirmed. In our study, both depots showed equal sensitivity to insulin stimulation on glucose uptake, which has also been shown in other reports (Westergren, Danielsson et al. 2005). We also showed that glucose levels in blood was associated with reduced glucose uptake, which was most prominent in SAT. However, the associations did not reach significance, and we found no association between insulin sensitivity on glucose uptake with glucose level in blood. It should be emphasized that muscle tissue are responsible for most

(75-80%) of total body glucose uptake, and that adipose tissue only account for a smaller fraction of total body glucose uptake, leading to the conclusion that investigating glucose uptake in adipose tissue independently not necessarily explain glucose intolerance at systemic level (Honka, Latva-Rasku et al. 2018). Numerous studies have reported that an increased tendency to store fat in VAT are more detrimental to health, and it has been pointed on the fact that this fat depot are drained by the portal circulation causing free fatty acids to reach the liver in high concentrations (Rebuffe-Scrive, Andersson et al. 1989). Consequently, it is reasonable to believe that an elevated lipolysis in VAT relative to SAT is associated with a worsened metabolic profile. We found that stimulated lipolysis is significantly higher in VAT than SAT of obese subjects, which is also confirmed in other reports, and suggests that increased VAT mass has the potential to cause a marked exposure of the liver to free fatty acids via the portal drainage (Rebuffe-Scrive, Andersson et al. 1989). It has been reported a strong association of lipolysis and insulin resistance, and the lipolytic response to β-adrenergic stimulation is reported to be increased in VAT and decreased in SAT in insulin resistant subjects (Morigny, Houssier et al. 2016). Moreover, follow-up studies of morbidly obese patients undergoing bariatric surgery has reported a positive association between reduction in lipolytic rate and improvement of insulin sensitivity (Girousse, Tavernier et al. 2013). In support to this, we found a strong negative association of the lipolytic response with insulin sensitivity in VAT. Unexpectedly, our data indicated a negative association of both basal and stimulated lipolytic rate with measures of insulin resistance (HOMA-IR), and a positive association of basal lipolysis with insulin sensitivity on glucose uptake in VAT. Moreover, BMI showed a non-significant negative association with lipolysis in bot SAT and VAT. However, it is important to emphasize that we measured lipolysis per volume fat mass, and did not take into account differences in distribution of fat mass between SAT and VAT. Considering the expanded fat volume of severely obese subjects, there is a much greater potential of causing harmful effects on metabolic health by ectopic lipid accumulation.

5.4 Summary, Limitations and future perspective

In summary, our data shows that macrophages are more abundant in SAT than VAT of obese subjects. Both flow cytometry data and gene expression analysis support an association of anti-inflammatory M2-like macrophages in SAT and insulin resistance and an association between systemic inflammation and inflammation in VAT. We should, however, be precautious when interpreting the correlation analysis of the flow cytometry data due to the limited sample size of 16 subjects. Moreover, the gene expression data are derived from whole tissue biopsies and thus represents the average expression level from many different cell types and are thereby not directly comparable with the flow cytometry data, which provide a more precise information of the cellular composition. Furthermore, it has been shown that TREM2 is also expressed by adipocytes and non-immune cells in the adipose tissue (Liu, Li et al. 2019). Moreover, limited access on lean healthy controls and the fact that one from the control group present with highest HOMA-IR, CRP levels and M1/M2 ratio limit the potential to perform a statistically meaningful analysis to assess whether obesity is associated with adipose tissue inflammation or insulin resistance. The fact that some patients are medically treated for T2DM to manage their glucose intolerance and insulin resistance brings further complexity to the analysis. In addition, the severely obese patients are encouraged to follow a caloric restrict diet the last weeks ahead of bariatric surgery, which may lead to weight loss and modulate the composition of macrophages and level of insulin sensitivity. Future studies should include a higher number of lean healthy controls and look more into how to best define different subsets of macrophages with the aim of investigating their role in adipose tissue inflammation and insulin resistance.

References

(2016). "Correction for Lee et al., Shox2 is a molecular determinant of depot-specific adipocyte function." Proc Natl Acad Sci U S A **113**(16): E2347.

Apovian, C. M. (2016). "Obesity: definition, comorbidities, causes, and burden." Am J Manag Care **22**(7 Suppl): s176-185.

Bastard, J. P., M. Maachi, J. T. Van Nhieu, C. Jardel, E. Bruckert, A. Grimaldi, J. J. Robert, J. Capeau and B. Hainque (2002). "Adipose tissue IL-6 content correlates with resistance to insulin activation of glucose uptake both in vivo and in vitro." J Clin Endocrinol Metab **87**(5): 2084-2089.

Bodis, K. and M. Roden (2018). "Energy metabolism of white adipose tissue and insulin resistance in humans." Eur J Clin Invest **48**(11): e13017.

Boutens, L. and R. Stienstra (2016). "Adipose tissue macrophages: going off track during obesity." Diabetologia **59**(5): 879-894.

Burhans, M. S., D. K. Hagman, J. N. Kuzma, K. A. Schmidt and M. Kratz (2018). "Contribution of Adipose Tissue Inflammation to the Development of Type 2 Diabetes Mellitus." Compr Physiol **9**(1): 1-58.

Cancello, R., J. Tordjman, C. Poitou, G. Guilhem, J. L. Bouillot, D. Hugol, C. Coussieu, A. Basdevant, A. Bar Hen, P. Bedossa, M. Guerre-Millo and K. Clement (2006). "Increased infiltration of macrophages in omental adipose tissue is associated with marked hepatic lesions in morbid human obesity." Diabetes **55**(6): 1554-1561.

Chait, A. and L. J. den Hartigh (2020). "Adipose Tissue Distribution, Inflammation and Its Metabolic Consequences, Including Diabetes and Cardiovascular Disease." Front Cardiovasc Med **7**: 22.

Chen, H., M. Montagnani, T. Funahashi, I. Shimomura and M. J. Quon (2003). "Adiponectin stimulates production of nitric oxide in vascular endothelial cells." J Biol Chem **278**(45): 45021-45026.

Chondronikola, M., E. Volpi, E. Borsheim, C. Porter, P. Annamalai, S. Enerback, M. E. Lidell, M. K. Saraf, S. M. Labbe, N. M. Hurren, C. Yfanti, T. Chao, C. R. Andersen, F. Cesani, H. Hawkins and L. S. Sidossis (2014). "Brown adipose tissue improves whole-body glucose homeostasis and insulin sensitivity in humans." Diabetes **63**(12): 4089-4099.

Chooi, Y. C., C. Ding and F. Magkos (2019). "The epidemiology of obesity." Metabolism **92**: 6-10.

Christen, T., Y. Sheikine, V. Z. Rocha, S. Hurwitz, A. B. Goldfine, M. Di Carli and P. Libby (2010). "Increased glucose uptake in visceral versus subcutaneous adipose tissue revealed by PET imaging." JACC Cardiovasc Imaging **3**(8): 843-851.

Cinti, S., G. Mitchell, G. Barbatelli, I. Murano, E. Ceresi, E. Faloia, S. Wang, M. Fortier, A. S. Greenberg and M. S. Obin (2005). "Adipocyte death defines macrophage localization and function in adipose tissue of obese mice and humans." J Lipid Res **46**(11): 2347-2355.

Collaboration, N. C. D. R. F. (2016). "Worldwide trends in diabetes since 1980: a pooled analysis of 751 population-based studies with 4.4 million participants." Lancet **387**(10027): 1513-1530.

Devaraj, S. and I. Jialal (2011). "C-reactive protein polarizes human macrophages to an M1 phenotype and inhibits transformation to the M2 phenotype." Arterioscler Thromb Vasc Biol **31**(6): 1397-1402.

Etzerodt, A. and S. K. Moestrup (2013). "CD163 and inflammation: biological, diagnostic, and therapeutic aspects." Antioxid Redox Signal **18**(17): 2352-2363.

Fay, L., A. Carll-White and K. Real (2018). "Emergency Nurses' Perceptions of Efficiency and Design: Examining ED Structure, Process, and Outcomes." J Emerg Nurs **44**(3): 274-279.

Fontana, L., J. C. Eagon, M. E. Trujillo, P. E. Scherer and S. Klein (2007). "Visceral fat adipokine secretion is associated with systemic inflammation in obese humans." Diabetes **56**(4): 1010-1013.

Gassaway, B. M., M. C. Petersen, Y. V. Surovtseva, K. W. Barber, J. B. Sheetz, H. R. Aerni, J. S. Merkel, V. T. Samuel, G. I. Shulman and J. Rinehart (2018). "PKCepsilon contributes to lipid-induced insulin resistance through cross talk with p70S6K and through previously unknown regulators of insulin signaling." Proc Natl Acad Sci U S A **115**(38): E8996-E9005.

Girousse, A., G. Tavernier, C. Valle, C. Moro, N. Mejhert, A. L. Dinel, M. Houssier, B. Roussel, A. Besse-Patin, M. Combes, L. Mir, L. Monbrun, V. Bezaire, B. Prunet-Marcassus, A. Waget, I. Vila, S. Caspar-Bauguil, K. Louche, M. A. Marques, A. Mairal, M. L. Renoud, J. Galitzky, C. Holm, E. Mouisel, C. Thalamas, N. Viguerie, T. Sulpice, R. Burcelin, P. Arner and D. Langin (2013). "Partial inhibition of adipose tissue lipolysis improves glucose metabolism and insulin sensitivity without alteration of fat mass." PLoS Biol **11**(2): e1001485.

Goodarzi, M. O. (2018). "Genetics of obesity: what genetic association studies have taught us about the biology of obesity and its complications." Lancet Diabetes Endocrinol **6**(3): 223-236.

Hagman, D. K., J. N. Kuzma, I. Larson, K. E. Foster-Schubert, L. Y. Kuan, A. Cignarella, E. Geamanu, K. W. Makar, J. R. Gottlieb and M. Kratz (2012). "Characterizing and quantifying leukocyte populations in human adipose tissue: impact of enzymatic tissue processing." J Immunol Methods **386**(1-2): 50-59.

Honka, M. J., A. Latva-Rasku, M. Bucci, K. A. Virtanen, J. C. Hannukainen, K. K. Kalliokoski and P. Nuutila (2018). "Insulin-stimulated glucose uptake in skeletal muscle, adipose tissue and liver: a positron emission tomography study." Eur J Endocrinol **178**(5): 523-531.

Huang, X., G. Liu, J. Guo and Z. Su (2018). "The PI3K/AKT pathway in obesity and type 2 diabetes." Int J Biol Sci **14**(11): 1483-1496.

Hurtado del Pozo, C., R. M. Calvo, G. Vesperinas-Garcia, J. Gomez-Ambrosi, G. Fruhbeck, R. Corripio-Sanchez, M. A. Rubio and M. J. Obregon (2010). "IPO8 and FBXL10: new reference genes for gene expression studies in human adipose tissue." Obesity (Silver Spring) **18**(5): 897-903.

Iacobini, C., G. Pugliese, C. Blasetti Fantauzzi, M. Federici and S. Menini (2019). "Metabolically healthy versus metabolically unhealthy obesity." Metabolism **92**: 51-60.

Jaitin, D. A., L. Adlung, C. A. Thaiss, A. Weiner, B. Li, H. Descamps, P. Lundgren, C. Bleriot, Z. Liu, A. Deczkowska, H. Keren-Shaul, E. David, N. Zmora, S. M. Eldar, N. Lubezky, O. Shibolet, D. A. Hill, M. A. Lazar, M. Colonna, F. Ginhoux, H. Shapiro, E. Elinav and I. Amit (2019). "Lipid-Associated Macrophages Control Metabolic Homeostasis in a Trem2-Dependent Manner." Cell **178**(3): 686-698 e614.

Kahn, S. E., M. E. Cooper and S. Del Prato (2014). "Pathophysiology and treatment of type 2 diabetes: perspectives on the past, present, and future." Lancet **383**(9922): 1068-1083.

Kanda, H., S. Tateya, Y. Tamori, K. Kotani, K. Hiasa, R. Kitazawa, S. Kitazawa, H. Miyachi, S. Maeda, K. Egashira and M. Kasuga (2006). "MCP-1 contributes to macrophage infiltration into adipose tissue, insulin resistance, and hepatic steatosis in obesity." J Clin Invest **116**(6): 1494-1505.

Kang, H. S., G. Liao, L. M. DeGraff, K. Gerrish, C. D. Bortner, S. Garantziotis and A. M. Jetten (2013). "CD44 plays a critical role in regulating diet-induced adipose inflammation, hepatic steatosis, and insulin resistance." PLoS One **8**(3): e58417.

Karamohamed, S., S. Demissie, J. Volcjak, C. Liu, N. Heard-Costa, J. Liu, C. M. Shoemaker, C. I. Panhuysen, J. B. Meigs, P. Wilson, L. D. Atwood, L. A. Cupples, A. Herbert and N. F. H. Study (2003). "Polymorphisms in the insulin-degrading enzyme gene are associated with type 2 diabetes in men from the NHLBI Framingham Heart Study." Diabetes **52**(6): 1562-1567.

Kelley, S. L., T. Lukk, S. K. Nair and R. I. Tapping (2013). "The crystal structure of human soluble CD14 reveals a bent solenoid with a hydrophobic amino-terminal pocket." J Immunol **190**(3): 1304-1311.

Kennedy, A., K. Martinez, C. C. Chuang, K. LaPoint and M. McIntosh (2009). "Saturated fatty acid-mediated inflammation and insulin resistance in adipose tissue: mechanisms of action and implications." J Nutr **139**(1): 1-4.

Kershaw, E. E. and J. S. Flier (2004). "Adipose tissue as an endocrine organ." J Clin Endocrinol Metab **89**(6): 2548-2556.

Kim, H. H., Y. Zhang and A. Heller (2004). "Bilirubin oxidase label for an enzyme-linked affinity assay with O2 as substrate in a neutral pH NACL solution." Anal Chem **76**(8): 2411-2414.

Kim, J., K. Chung, C. Choi, J. Beloor, I. Ullah, N. Kim, K. Y. Lee, S. K. Lee and P. Kumar (2016). "Silencing CCR2 in Macrophages Alleviates Adipose Tissue Inflammation and the Associated Metabolic Syndrome in Dietary Obese Mice." Mol Ther Nucleic Acids **5**: e280.

Kim, M., M. H. Seol and B. C. Lee (2019). "The Effects of Poncirus fructus on Insulin Resistance and the Macrophage-Mediated Inflammatory Response in High Fat Diet-Induced Obese Mice." Int J Mol Sci **20**(12).

Klover, P. J., T. A. Zimmers, L. G. Koniaris and R. A. Mooney (2003). "Chronic exposure to interleukin-6 causes hepatic insulin resistance in mice." Diabetes **52**(11): 2784-2789.

Koenen, T. B., R. Stienstra, L. J. van Tits, L. A. Joosten, J. F. van Velzen, A. Hijmans, J. A. Pol, J. A. van der Vliet, M. G. Netea, C. J. Tack, A. F. Stalenhoef and J. de Graaf (2011). "The inflammasome and caspase-1 activation: a new mechanism underlying increased inflammatory activity in human visceral adipose tissue." Endocrinology **152**(10): 3769-3778.

Kubota, N., Y. Terauchi, T. Yamauchi, T. Kubota, M. Moroi, J. Matsui, K. Eto, T. Yamashita, J. Kamon, H. Satoh, W. Yano, P. Froguel, R. Nagai, S. Kimura, T. Kadowaki and T. Noda (2002). "Disruption of adiponectin causes insulin resistance and neointimal formation." J Biol Chem **277**(29): 25863-25866.

Kurauti, M. A., J. M. Costa-Junior, S. M. Ferreira, G. J. Santos, C. H. G. Sponton, E. M. Carneiro, G. D. Telles, M. P. T. Chacon-Mikahil, C. R. Cavaglieri, L. F. Rezende and A. C. Boschero (2017). "Interleukin-6 increases the expression and activity of insulin-degrading enzyme." Sci Rep **7**: 46750.

Lass, A., R. Zimmermann, M. Oberer and R. Zechner (2011). "Lipolysis - a highly regulated multi-enzyme complex mediates the catabolism of cellular fat stores." Prog Lipid Res **50**(1): 14-27.

Lebovitz, H. E. and M. A. Banerji (2005). "Point: visceral adiposity is causally related to insulin resistance." Diabetes Care **28**(9): 2322-2325.

Lim, S. Y., A. E. Yuzhalin, A. N. Gordon-Weeks and R. J. Muschel (2016). "Targeting the CCL2-CCR2 signaling axis in cancer metastasis." Oncotarget **7**(19): 28697-28710.

Liu, C., P. Li, H. Li, S. Wang, L. Ding, H. Wang, H. Ye, Y. Jin, J. Hou, X. Fang and Q. Shu (2019). "TREM2 regulates obesity-induced insulin resistance via adipose tissue remodeling in mice of high-fat feeding." J Transl Med **17**(1): 300.

Mantovani, A., A. Sica, S. Sozzani, P. Allavena, A. Vecchi and M. Locati (2004). "The chemokine system in diverse forms of macrophage activation and polarization." Trends Immunol **25**(12): 677-686.

Mark, A. L. (2013). "Selective leptin resistance revisited." Am J Physiol Regul Integr Comp Physiol **305**(6): R566-581.

Martyniak, K. and M. M. Masternak (2017). "Changes in adipose tissue cellular composition during obesity and aging as a cause of metabolic dysregulation." Exp Gerontol **94**: 59-63.

Mauer, J., B. Chaurasia, J. Goldau, M. C. Vogt, J. Ruud, K. D. Nguyen, S. Theurich, A. C. Hausen, J. Schmitz, H. S. Bronneke, E. Estevez, T. L. Allen, A. Mesaros, L. Partridge, M. A. Febbraio, A. Chawla, F.

T. Wunderlich and J. C. Bruning (2014). "Signaling by IL-6 promotes alternative activation of macrophages to limit endotoxemia and obesity-associated resistance to insulin." Nat Immunol **15**(5): 423-430.

Mauer, J., J. L. Denson and J. C. Bruning (2015). "Versatile functions for IL-6 in metabolism and cancer." Trends Immunol **36**(2): 92-101.

Midthjell, K., C. M. Lee, A. Langhammer, S. Krokstad, T. L. Holmen, K. Hveem, S. Colagiuri and J. Holmen (2013). "Trends in overweight and obesity over 22 years in a large adult population: the HUNT Study, Norway." Clin Obes **3**(1-2): 12-20.

Morgan-Bathke, M., D. Harteneck, P. Jaeger, E. Sondergaard, R. Karwoski, A. Espinosa De Ycaza, B. G. Carranza-Leon, W. A. Faubion, Jr., A. M. Oliveira and M. D. Jensen (2017). "Comparison of Methods for Analyzing Human Adipose Tissue Macrophage Content." Obesity (Silver Spring) **25**(12): 2100-2107.

Morigny, P., M. Houssier, E. Mouisel and D. Langin (2016). "Adipocyte lipolysis and insulin resistance." Biochimie **125**: 259-266.

Murawska-Cialowicz, E. (2017). "Adipose tissue - morphological and biochemical characteristic of different depots." Postepy Hig Med Dosw (Online) **71**(0): 466-484.

Nawrocki, A. R., M. W. Rajala, E. Tomas, U. B. Pajvani, A. K. Saha, M. E. Trumbauer, Z. Pang, A. S. Chen, N. B. Ruderman, H. Chen, L. Rossetti and P. E. Scherer (2006). "Mice lacking adiponectin show decreased hepatic insulin sensitivity and reduced responsiveness to peroxisome proliferator-activated receptor gamma agonists." J Biol Chem **281**(5): 2654-2660.

O'Rourke, R. W., A. E. White, M. D. Metcalf, B. R. Winters, B. S. Diggs, X. Zhu and D. L. Marks (2012). "Systemic inflammation and insulin sensitivity in obese IFN-gamma knockout mice." Metabolism **61**(8): 1152-1161.

Ouchi, N. and K. Walsh (2007). "Adiponectin as an anti-inflammatory factor." Clin Chim Acta **380**(1-2): 24-30.

Pahlavani, M., T. Ramalho, I. Koboziev, M. J. LeMieux, S. Jayarathne, L. Ramalingam, L. R. Filgueiras and N. Moustaid-Moussa (2017). "Adipose tissue inflammation in insulin resistance: review of mechanisms mediating anti-inflammatory effects of omega-3 polyunsaturated fatty acids." J Investig Med **65**(7): 1021-1027.

Pasarica, M., H. Xie, D. Hymel, G. Bray, F. Greenway, E. Ravussin and S. R. Smith (2009). "Lower total adipocyte number but no evidence for small adipocyte depletion in patients with type 2 diabetes." Diabetes Care **32**(5): 900-902.

Patsouris, D., P. P. Li, D. Thapar, J. Chapman, J. M. Olefsky and J. G. Neels (2008). "Ablation of CD11c-positive cells normalizes insulin sensitivity in obese insulin resistant animals." Cell Metab **8**(4): 301-309.

Pedersen, B. K. and C. P. Fischer (2007). "Beneficial health effects of exercise--the role of IL-6 as a myokine." Trends Pharmacol Sci **28**(4): 152-156.
Petersen, M. C. and G. I. Shulman (2018). "Mechanisms of Insulin Action and Insulin Resistance." Physiol Rev **98**(4): 2133-2223.
Pilgaard, L., P. Lund, J. G. Rasmussen, T. Fink and V. Zachar (2008). "Comparative analysis of highly defined proteases for the isolation of adipose tissue-derived stem cells." Regen Med **3**(5): 705-715.
Rebuffe-Scrive, M., B. Andersson, L. Olbe and P. Bjorntorp (1989). "Metabolism of adipose tissue in intraabdominal depots of nonobese men and women." Metabolism **38**(5): 453-458.
Ruiz, P. L. D., L. C. Stene, I. J. Bakken, S. E. Haberg, K. I. Birkeland and H. L. Gulseth (2018). "Decreasing incidence of pharmacologically and non-pharmacologically treated type 2 diabetes in Norway: a nationwide study." Diabetologia **61**(11): 2310-2318.
Saely, C. H., K. Geiger and H. Drexel (2012). "Brown versus white adipose tissue: a mini-review." Gerontology **58**(1): 15-23.
Scheen, A. J. (2003). "Pathophysiology of type 2 diabetes." Acta Clin Belg **58**(6): 335-341.
Senbanjo, L. T. and M. A. Chellaiah (2017). "CD44: A Multifunctional Cell Surface Adhesion Receptor Is a Regulator of Progression and Metastasis of Cancer Cells." Front Cell Dev Biol **5**: 18.
Stolarczyk, E. (2017). "Adipose tissue inflammation in obesity: a metabolic or immune response?" Curr Opin Pharmacol **37**: 35-40.
Szymczak-Pajor, I. and A. Sliwinska (2019). "Analysis of Association between Vitamin D Deficiency and Insulin Resistance." Nutrients **11**(4).
Turnbull, I. R., S. Gilfillan, M. Cella, T. Aoshi, M. Miller, L. Piccio, M. Hernandez and M. Colonna (2006). "Cutting edge: TREM-2 attenuates macrophage activation." J Immunol **177**(6): 3520-3524.
Vats, D., L. Mukundan, J. I. Odegaard, L. Zhang, K. L. Smith, C. R. Morel, R. A. Wagner, D. R. Greaves, P. J. Murray and A. Chawla (2006). "Oxidative metabolism and PGC-1beta attenuate macrophage-mediated inflammation." Cell Metab **4**(1): 13-24.
Wang, Q. A., C. Tao, R. K. Gupta and P. E. Scherer (2013). "Tracking adipogenesis during white adipose tissue development, expansion and regeneration." Nat Med **19**(10): 1338-1344.
Wentworth, J. M., G. Naselli, W. A. Brown, L. Doyle, B. Phipson, G. K. Smyth, M. Wabitsch, P. E. O'Brien and L. C. Harrison (2010). "Pro-inflammatory CD11c+CD206+ adipose tissue macrophages are associated with insulin resistance in human obesity." Diabetes **59**(7): 1648-1656.
Westergren, H., A. Danielsson, F. H. Nystrom and P. Stralfors (2005). "Glucose transport is equally sensitive to insulin stimulation, but basal and insulin-stimulated transport is higher, in human omental compared with subcutaneous adipocytes." Metabolism **54**(6): 781-785.

Yilmaz, M. B., S. F. Biyikoglu, Y. Akin, U. Guray, H. L. Kisacik and S. Korkmaz (2003). "Obesity is associated with impaired coronary collateral vessel development." Int J Obes Relat Metab Disord **27**(12): 1541-1545.

Zhang, Y., A. J. Federation, S. Kim, J. P. O'Keefe, M. Lun, D. Xiang, J. D. Brown and M. L. Steinhauser (2018). "Targeting nuclear receptor NR4A1-dependent adipocyte progenitor quiescence promotes metabolic adaptation to obesity." J Clin Invest **128**(11): 4898-4911.

Zhang, Y., L. Xie, S. K. Gunasekar, D. Tong, A. Mishra, W. J. Gibson, C. Wang, T. Fidler, B. Marthaler, A. Klingelhutz, E. D. Abel, I. Samuel, J. K. Smith, L. Cao and R. Sah (2017). "SWELL1 is a regulator of adipocyte size, insulin signalling and glucose homeostasis." Nat Cell Biol **19**(5): 504-517.

Zhong, L., X. F. Chen, Z. L. Zhang, Z. Wang, X. Z. Shi, K. Xu, Y. W. Zhang, H. Xu and G. Bu (2015). "DAP12 Stabilizes the C-terminal Fragment of the Triggering Receptor Expressed on Myeloid Cells-2 (TREM2) and Protects against LPS-induced Pro-inflammatory Response." J Biol Chem **290**(25): 15866-15877.

Supplementary

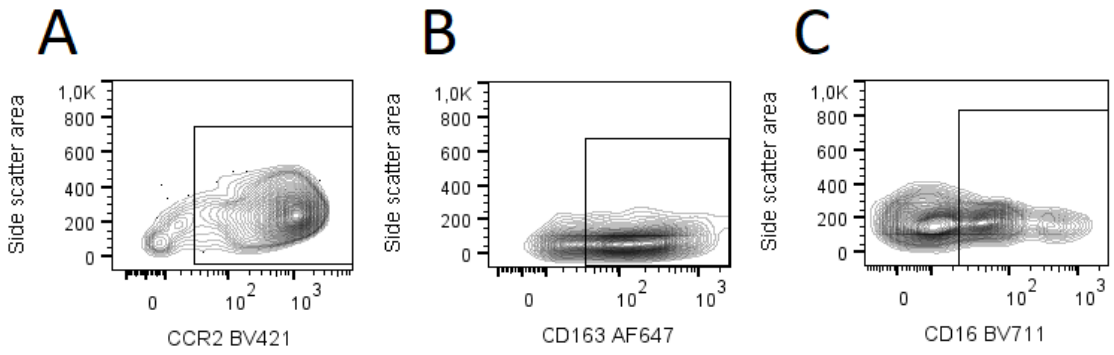

Figure 1. Gating strategy for quantification of CCR2, CD163 and CD16 expressing cells. *The gating strategy for quantifying the fraction of Monocytes, M1- and M2-like macrophages expressing the receptors CCR2 (A), CD163 (B) and CD16 (C) from one representative population.*